mathematics

Article

Study of Stochastic–Fractional Drinfel'd–Sokolov–Wilson Equation for M-Shaped Rational, Homoclinic Breather, Periodic and Kink-Cross Rational Solutions

Shami A. M. Alsallami [1], Syed T. R. Rizvi [2] and Aly R. Seadawy [3,*]

[1] Department of Mathematical Sciences, College of Applied Science, Umm Al-Qura University, Makkah 21955, Saudi Arabia
[2] Department of Mathematics, COMSATS University Islamabad, Lahore Campus, Lahore 54840, Pakistan
[3] Mathematics Department, Faculty of Science, Taibah University, Al-Madinah Al-Munawarah 41411, Saudi Arabia
* Correspondence: aabdelalim@taibahu.edu.sa

Abstract: We explore stochastic–fractional Drinfel'd–Sokolov–Wilson (SFDSW) equations for some wave solutions such as the cross-kink rational wave solution, periodic cross-rational wave solution and homoclinic breather wave solution. We also examine some M-shaped solutions such as the M-shaped rational solution, M-shaped rational solution with one and two kink waves. We also derive the M-shaped interaction with rogue and kink waves and the M-shaped interaction with periodic and kink waves. This model is used in mathematical physics, surface physics, plasma physics, population dynamics and applied sciences. Moreover, we also show our results graphically in different dimensions. We obtain these solutions under some constraint conditions.

Keywords: breathers; periodic cross-kink; homoclinic breather; M-shaped solution; cross-kink rational solution

MSC: 35R10; 35R11

check for updates

Citation: Alsallami, S.A.M.; Rizvi, S.T.R.; Seadawy, A.R. Study of Stochastic–Fractional Drinfel'd–Sokolov–Wilson Equation for M-Shaped Rational, Homoclinic Breather, Periodic and Kink-Cross Rational Solutions. *Mathematics* **2023**, *11*, 1504. https://doi.org/10.3390/math11061504

Academic Editor: Panayiotis Vafeas

Received: 17 January 2023
Revised: 2 March 2023
Accepted: 9 March 2023
Published: 20 March 2023

Copyright: © 2023 by the authors. Licensee MDPI, Basel, Switzerland. This article is an open access article distributed under the terms and conditions of the Creative Commons Attribution (CC BY) license (https://creativecommons.org/licenses/by/4.0/).

1. Introduction

Numerous branches of nonlinear science including plasma physics, geochemistry, solid-state physics, fluid mechanics [1–4], optical fibres, nuclear physics and chemical physics have been studied through nonlinear evolution equations (NLEEs) [5–8]. The travelling-wave solution for NLEEs executes a number of analytical and numerical techniques to get an exact solution for these NLEEs [9–15]. Recently, a variety of external stimulations including random disturbances have been involved in changing physical systems.

A stochastic differential equation (SDE) is a differential equation that has one or more stochastic processes as its terms, with the solution being another stochastic process. SDEs are used to simulate a variety of phenomena, including stock prices and physical models subject to thermal fluctuating. Consequently, SDEs have emerged and gained a lot of significance in modelling phenomena in atmospheric science, fluid mechanics, oceanography, chemistry, physics and biology [16,17].

The fractional derivative models are used for the accurate modelling of those systems that require an accurate modelling of the damping. The advantages of fractional derivatives are their flexibility and nonlocality. These derivatives can approximate real data with a greater flexibility than classical derivatives because they are of fractional order. Moreover, they consider nonlocality, which classical derivatives are unable to achieve. However, a number of significant phenomena such as anomalous diffusion, electrochemistry, acoustics, image processing and electromagnetism are represented by fractional derivative. Fractional models are more precise than integer models. In general, it is more challenging to obtain an exact solution of SDEs with fractional derivatives than classical ones. As a result, we considered the following SFDSW equations given as [18]:

$$du + [\beta_1 v D_x^{\omega} v]dt = \zeta u d\eta, \tag{1}$$

$$dv + [\beta_2 D_{xxx}^{\omega} v + \beta_3 u D_x^{\omega} v + \beta_4 v D_x^{\omega} u]dt = \zeta v d\eta, \tag{2}$$

where $u = u(x,t)$, $v = v(x,t)$ and β_j for $j = 1,2,3,4$ are nonzero constant. $\eta = \eta(t)$ is the standard Brownian motion, ζ is noise strength, and D^{ω} is a conformable derivative for $0 < \omega < 1$.

The remaining manuscript is arranged as follows: In Section 2, we explain the properties and definitions of standard Brownian motion and also discuss Hirota's bilinear method. In Section 3, we obtain the wave equation for the SFDSW equation. In Sections 4 and 5, we introduce the solution for the cross-kink rational solution and periodic cross-rational solution, respectively; we also examine the homoclinic breather in Section 6, M-shaped rational wave solution in Section 7, M-shaped rational wave solution with one kink and two kink waves in Sections 8 and 9, respectively. Moreover, we obtain the M-shaped rational interaction with rogue and kink waves and the M-shaped rational interaction with periodic and kink waves in Sections 10 and 11. In Section 12, we address results and discussion. Section 13 presents the conclusion of the paper.

2. Preliminaries

Now, we discuss the properties and definitions of a conformable derivative and standard Brownian motion. The definition of a conformable derivative is given as:

Definition 1 ([19]). *The conformable derivative with order ω of $Q : R^+ \to R$ is given as:*

$$D_x^{\omega} Q(z) = \lim_{m \to 0} \frac{Q(z + mz^{1-\omega}) - Q(z)}{m}.$$

Theorem 1 ([19]). *Suppose that $Q_1, Q_2 : R^+ \to R$ are ω differential functions,*

$$D_x^{\omega}(Q_1 \, o \, Q_2)(z) = z^{1-\omega} Q_2'(x) Q_1(Q_2(x)).$$

Some properties of the conformable derivative are given as:
1. $D_z^{\omega}[n_1 Q_1(z) + n_2 Q_2(z)] = n_1 D_x^{\omega} Q_1(z) + n_2 D_x^{\omega} Q_2(z),\ n_1,\ n_2 \epsilon R;$
2. $D_z^{\omega}[z^m] = m z^{m-\omega},\ m \epsilon R;$
3. $D_z^{\omega} Q(x) = z^{1-\omega} \frac{dQ}{dx};$
4. $D_z^{\omega}[K] = 0$, K is constant.

Definition 2 ([20]). *A stochastic system $\{\eta(t)\}_{t \geq 0}$ is a standard Brownian motion if*

1. $\eta(0) = 0$,
2. $\eta(t),\ t \geq 0$, is a continuous function of t;
3. $\eta(t_1) - \eta(t_2)$ is independent for $t_1 < t_2$;
4. With the variance $t_2 - t_1$ and mean 0, $\eta(t_2) - \eta(t_1)$ has a normal distribution.

Lemma 1 ([20]). $E(e^{\gamma \eta(t)}) = e^{\frac{1}{2}\gamma^2 t}$ for $\gamma \geq 0$.

Hirota's Bilinear Method

Hirota invented a method in 1971 to obtain multisoliton solutions of integrable nonlinear evolution equations. A particularly simple manifestation of multisoliton solutions was desired, therefore the aim was to convert existing variables into new ones. Hirota's method was the quickest to provide results to find soliton solutions [21].

The standard definition of Hirota's bilinear operators was first introduced by Hirota as:

$$D_t^n D_x^m(\alpha.\beta) = (\frac{\partial}{\partial t} - \frac{\partial}{\partial t'})^n(\frac{\partial}{\partial x} - \frac{\partial}{\partial x'})^m \alpha(x,t)\beta(x',t') \mid x' = x, t' = t'.$$

This type of equations can typically be made bilinear by including a new dependent variable, such as $\log f$ or $\frac{f}{g}$.

3. Wave Transformation for SFDSW

For SFDSW Equations (1) and (2), we use the following wave transformation to build the wave equation [18]:

$$u(x,t) = U(\nu)e^{(\zeta\eta(t)-\frac{1}{2}\zeta^2 t)},\ v(x,t) = V(\nu)e^{(\zeta\eta(t)-\frac{1}{2}\zeta^2 t)},\ \nu = \frac{1}{\omega}x^\omega + \phi t, \tag{3}$$

where U and V are real functions. Inserting Equation (3) into Equations (1) and (2), we have

$$\begin{aligned} du &= [\phi U' dt + \zeta U d\eta]e^{(\zeta\eta(t)-\frac{1}{2}\zeta^2 t)}, \\ dv &= [\phi V' dt + \zeta V d\eta]e^{(\zeta\eta(t)-\frac{1}{2}\zeta^2 t)}, \\ D_x^\omega v &= V' e^{(\zeta\eta(t)-\frac{1}{2}\zeta^2 t)}, \\ D_x^\omega u &= U' e^{(\zeta\eta(t)-\frac{1}{2}\zeta^2 t)}, \\ D_{xxx}^\omega v &= V''' e^{(\zeta\eta(t)-\frac{1}{2}\zeta^2 t)}. \end{aligned} \tag{4}$$

By using Equation (4) into Equations (1) and (2), we get

$$\phi U' + \beta_1 V V' e^{(\zeta\eta(t)-\frac{1}{2}\zeta^2 t)} = 0, \tag{5}$$

$$\phi V' + \beta_2 V''' + \beta_3 U V' e^{(\zeta\eta(t)-\frac{1}{2}\zeta^2 t)} + \beta_4 V U' e^{(\zeta\eta(t)-\frac{1}{2}\zeta^2 t)} = 0, \tag{6}$$

and we have

$$\phi U' + \beta_1 V V' e^{-\frac{1}{2}\zeta^2 t} E(e^\zeta \eta(t)) = 0, \tag{7}$$

$$\phi V' + \beta_2 V''' + [\beta_3 U V' + \beta_4 V U'] e^{-\frac{1}{2}\zeta^2 t} E(e^\zeta \eta(t)) = 0. \tag{8}$$

Using Lemma 1, we have

$$\phi U' + \beta_1 V V' = 0, \tag{9}$$

$$\phi V' + \beta_2 V''' + \beta_3 U V' + \beta_4 V U' = 0. \tag{10}$$

Integrating Equation (9), we obtain

$$U = -\frac{\beta_1}{\phi} V^2 + C, \tag{11}$$

where C is a constant. Inserting Equation (11) into Equation (10), and utilizing Equation (9), we obtain

$$\beta_2 V''' - [\frac{\beta_1\beta_3}{2\phi} + \frac{\beta_1\beta_4}{\phi}] V^2 V' + [\phi + C\beta_3] V' = 0. \tag{12}$$

Integrating Equation (12), we have the following wave equation

$$V'' - h_1 V^3 + h_2 V = 0, \tag{13}$$

where $h_1 = \frac{\beta_1\beta_3}{6\beta_2\phi} + \frac{\beta_1\beta_4}{3\beta_2\phi}$ and $h_2 = \frac{\phi}{\beta_2} + \frac{C\beta_3}{\beta_2}$. To find the bilinear form of Equation (13), we substitute the following transformation for various solutions [22]:

$$V = 2(\log f)_\nu, \tag{14}$$

$$6\beta_3 C\phi f^2 f' + 6\beta_2\phi f^2 f^{(3)} + 12\beta_2\phi f'^3 - 4\beta_1\beta_3 f'^3 - 8\beta_1\beta_4 f'^3 + 6\phi^2 f^2 f' - 18\beta_2\phi f f' f''. \tag{15}$$

Now, we study the following wave solution by using Equation (15):

4. Cross-Kink Rational Wave Solution

We use the following ansatz for the cross-kink rational wave [23]:

$$\begin{gathered} f = e^{-G_1} + r_1 e^{G_1} + c_1^2 + c_2^2 + w_5, \\ c_1 = w_1\nu + w_2, \qquad c_2 = w_3\nu + w_4, \\ G_1 = l_1\nu + l_2. \end{gathered} \tag{16}$$

Substitute Equation (16) into Equation (15). By equating the coefficients of x, $te^{-3l_1\nu-3l_2}$, $e^{-2l_1\nu-2l_2}$, $e^{-l_1\nu-l_2}$, $e^{l_1\nu+l_2}$, $e^{2l_1\nu+2l_2}$, $e^{3l_1\nu+3l_2}$, $e^{2(l_1\nu+l_2)-l_1\nu-l_2}$, $e^{2(l_1\nu+l_2)+l_1\nu+l_2}$ and $e^{2(l_1\nu+l_2)-2l_1\nu-2l_2}$ to zero, we have some values for the wave solution:

$$\begin{gathered} l_1 = 0, w_1 = -\frac{w_3 w_4}{w_2}, \\ w_5 = -\frac{\beta_3 C w_2^4 + \beta_3 C w_2^2 w_4^2 + w_2^4\phi - 3\beta_2 w_2^2 w_3^2 + w_2^2 w_4^2\phi - 3\beta_2 w_3^2 w_4^2}{w_2^2(\beta_3 C + \phi)}. \end{gathered} \tag{17}$$

Putting Equation (17) into Equation (16) and by using them Equation (14), we obtain

$$V = \frac{2\left(2w_3(\nu w_3 + w_4) - \frac{2w_3 w_4\left(w_2 - \frac{\nu w_3 w_4}{w_2}\right)}{w_2}\right)}{\Xi + e^{l_2} r_1 + e^{-l_2} + \left(w_2 - \frac{\nu w_3 w_4}{w_2}\right)^2 + (\nu w_3 + w_4)^2}. \tag{18}$$

Putting Equation (18) into Equation (11) yields

$$U = -\frac{4\beta_1 C\left(2w_3(\nu w_3 + w_4) - \frac{2w_3 w_4\left(w_2 - \frac{\nu w_3 w_4}{w_2}\right)}{w_2}\right)^2}{\phi\left(\Xi + e^{l_2} r_1 + e^{-l_2} + \left(w_2 - \frac{\nu w_3 w_4}{w_2}\right)^2 + (\nu w_3 + w_4)^2\right)^2}. \tag{19}$$

Inserting Equations (18) and (19) into Equation (3), we have

$$u(x,t) = -\frac{4\beta_1 C e^{\zeta\eta(t) - \frac{\zeta^2 t}{2}}\left(2w_3(\Delta) - \frac{2w_3 w_4(\Theta)}{w_2}\right)^2}{\phi\left(\Xi + e^{l_2} r_1 + e^{-l_2} + (\Theta)^2 + \left(w_3\left(t\phi + \frac{x^\omega}{\omega}\right) + w_4\right)^2\right)^2}, \tag{20}$$

$$v(x,t) = \frac{2e^{\zeta\eta(t) - \frac{\zeta^2 t}{2}}\left(2w_3(\Delta) - \frac{2w_3 w_4(\Theta)}{w_2}\right)}{\Xi + e^{l_2} r_1 + e^{-l_2} + (\Theta)^2 + (\Delta)^2}, \tag{21}$$

where $\Delta = w_3\left(t\phi + \frac{x^\omega}{\omega}\right) + w_4$, $\Theta = w_2 - \frac{w_3 w_4\left(t\phi + \frac{x^\omega}{\omega}\right)}{w_2}$ $\Xi = \frac{\beta_3(-C)w_2^4 - \beta_3 C w_2^2 w_4^2 - w_2^4\phi + 3\beta_2 w_2^2 w_3^2 - w_2^2 w_4^2\phi + 3\beta_2 w_3^2 w_4^2}{w_2^2(\beta_3 C + \phi)}$.

5. Periodic Cross-Rational Wave Solution

For periodic cross-rational waves, we utilize the given ansatz [24,25]:

$$f = c_1^2 + c_2^2 + r_1 \cos(G_1) + r_2 \cosh(G_2) + w_5, \tag{22}$$
$$a_1 = w_1 \nu + w_2, \qquad a_2 = w_3 \nu + w_4,$$
$$G_1 = l_1 \nu + l_2, \qquad G_2 = l_3 \nu + l_4.$$

Using Equation (22) into Equation (15) and zeroing the coefficients of $x, t \cos(l_1\nu + l_2)$, $\cos^2(l_1\nu + l_2), \cosh(l_3\nu + l_4), \cos(l_1\nu + l_2)\cosh(l_3\nu + l_4), \cosh^2(l_3\nu + l_4), \sin(l_1\nu + l_2)$, $\sin(l_1\nu + l_2)\cos(l_1\nu + l_2), \sin(l_1\nu + l_2)\cosh(l_3\nu + l_4), \sin(l_1\nu + l_2)\cos(l_1\nu + l_2)\cosh(l_3\nu + l_4), \sin(l_1\nu + l_2)\cosh^2(l_3\nu + l_4), \sinh(l_3\nu + l_4), \cos(l_1\nu + l_2)\sinh(l_3\nu + l_4)$, $\sinh(l_3\nu + l_4)\cosh(l_3\nu + l_4), \cos(l_1\nu + l_2)\sinh(l_3\nu + l_4)\cosh(l_3\nu + l_4)$, $\sinh(l_3\nu + l_4)\cosh^2(l_3\nu + l_4)$ and $\sinh^3(l_3\nu + l_4)$, we get some values for the periodic cross-rational wave solution:

$$l_3 = \sqrt{-\frac{\beta_3 C + \phi}{\beta_2}}, \; w_1 = -\frac{w_3 w_4}{w_2}, \tag{23}$$

Putting Equation (23) into Equation (22) and then inserting into Equation (14), we obtain

$$V = \frac{2\left(r_2\sqrt{\frac{\beta_3(-C)-\phi}{\beta_2}}\sinh(\varphi) - l_1 r_1 \sin(l_1\nu + l_2) - \frac{2w_3w_4\left(w_2 - \frac{\nu w_3 w_4}{w_2}\right)}{w_2} + 2w_3(\nu w_3 + w_4)\right)}{r_2\cosh(\varphi) + r_1\cos(l_1\nu + l_2) + \left(w_2 - \frac{\nu w_3 w_4}{w_2}\right)^2 + (\nu w_3 + w_4)^2 + w_5}. \tag{24}$$

Inserting Equation (24) into Equation (11) yields

$$U = -\frac{4\beta_1 C\left(r_2\sqrt{\frac{\beta_3(-C)-\phi}{\beta_2}}\sinh(\varphi) - l_1 r_1 \sin(l_1\nu + l_2) - \frac{2w_3w_4\left(w_2 - \frac{\nu w_3 w_4}{w_2}\right)}{w_2} + 2w_3(\nu w_3 + w_4)\right)^2}{\phi\left(r_2\cosh(\varphi) + r_1\cos(l_1\nu + l_2) + \left(w_2 - \frac{\nu w_3 w_4}{w_2}\right)^2 + (\nu w_3 + w_4)^2 + w_5\right)^2}, \tag{25}$$

where $\varphi = \nu\sqrt{\frac{\beta_3(-C)-\phi}{\beta_2}} + l_4$.

Substituting Equations (24) and (25) into Equation (3), we get

$$u(x,t) = -\frac{4\beta_1 C e^{\zeta\eta(t) - \frac{\zeta^2 t}{2}}\left(r_2\sqrt{\frac{\beta_3(-C)-\phi}{\beta_2}}\sinh(\Theta_1) - l_1 r_1 \sin(\Theta_2) - \frac{2w_3w_4(\Lambda)}{w_2} + 2w_3(\psi)\right)^2}{\phi\left(r_2\cosh(\Theta_1) + r_1\cos(\Theta_2) + (\Lambda)^2 + (\psi)^2 + w_5\right)^2}, \tag{26}$$

$$v(x,t) = \frac{2e^{\zeta\eta(t) - \frac{\zeta^2 t}{2}}\left(r_2\sqrt{\frac{\beta_3(-C)-\phi}{\beta_2}}\sinh(\Theta_1) - l_1 r_1 \sin(\Theta_2) - \frac{2w_3w_4(\Lambda)}{w_2} + 2w_3(\psi)\right)}{r_2\cosh(\Theta_1) + r_1\cos(\Theta_2) + (\Lambda)^2 + (\psi)^2 + w_5}, \tag{27}$$

where $\Theta_1 = \sqrt{\frac{\beta_3(-C)-\phi}{\beta_2}}\left(t\phi + \frac{x^\omega}{\omega}\right) + l_4$, $\Theta_2 = l_1\left(t\phi + \frac{x^\omega}{\omega}\right) + l_2$, $\Lambda = w_2 - \frac{w_3 w_4\left(t\phi + \frac{x^\omega}{\omega}\right)}{w_2}$ and $\psi = w_3\left(t\phi + \frac{x^\omega}{\omega}\right) + w_4$.

6. Homoclinic Breather Wave Solution

For homoclinic breather pulses, we use the following ansatz [26,27]:

$$f = e^{-w(l_1\nu + l_2)} + r_1 e^{l(w_3\nu + w_4)} + r_2\cos(w_1(l_5\nu + l_6)). \tag{28}$$

Putting Equation (28) into Equation (15), and setting the coefficients of $x, t, e^{-3w(l_1\nu+l_2)}$, $e^{w(l_3\nu+l_4)-2w(l_1\nu+l_2)}, e^{2w(l_3\nu+l_4)-w(l_1\nu+l_2)}, e^{3w(l_3\nu+l_4)}, e^{-2w(l_1\nu+l_2)}\cos(w_1(l_5\nu + l_6))$, $\cos(w_1(l_5\nu + l_6))e^{w(l_3\nu+l_4)-w(l_1\nu+l_2)}, e^{2w(l_3\nu+l_4)}\cos(w_1(l_5\nu + l_6)), e^{-w(l_1\nu+l_2)}$ $\cos^2(w_1(l_5\nu + l_6)), 6e^{w(l_3\nu+l_4)}\cos^2(w_1(l_5\nu + l_6)), e^{-2w(l_1\nu+l_2)}\sin(w_1(l_5\nu + l_6))$, $\sin(w_1(l_5\nu + l_6))e^{w(l_3\nu+l_4)-w(l_1\nu+l_2)}, e^{2w(l_3\nu+l_4)}\sin(w_1(l_5\nu + l_6))$, $e^{-w(l_1\nu+l_2)}\sin(w_1(l_5\nu + l_6))\cos(w_1(l_5\nu + l_6)), e^{w(l_3\nu+l_4)}\sin(w_1(l_5\nu + l_6))\cos(w_1(l_5\nu + l_6))$, $e^{-2w(l_1\nu+l_2)}\cos(w_1(l_5\nu + l_6)), \cos(w_1(l_5\nu + l_6))e^{w(l_3\nu+l_4)-w(l_1\nu+l_2)}$, $\cos(w_1(l_5\nu + l_6))e^{w(l_3\nu+l_4)-w(l_1\nu+l_2)}, \sin(w_1(l_5\nu + l_6))\cos^2(w_1(l_5\nu + l_6))$, $e^{-w(l_1\nu+l_2)}\sin^2(w_1(l_5\nu + l_6))$ and $e^{w(l_3\nu+l_4)}\sin^2(w_1(l_5\nu + l_6))$ to zero, we obtain the following for the homoclinic breather wave solution:

$$l_3 = 0, l_1 = \frac{\sqrt{-\frac{4\beta_3 C+4\phi}{\beta_2}}}{w},\ l_5 = \frac{\sqrt{-\frac{2\beta_3 C+2\phi}{\beta_2}}}{w_1}. \tag{29}$$

Using Equation (29) into Equation (28) and then using into Equation (14), we have

$$V = \frac{2\left(-\sqrt{\frac{-4\beta_3 C-4\phi}{\beta_2}}e^{-w\left(\frac{\nu\sqrt{\frac{-4\beta_3 C-4\phi}{\beta_2}}}{w}+l_2\right)} - r_2\sqrt{\frac{-2\beta_3 C-2\phi}{\beta_2}}\sin\left(w_1\left(\frac{\nu\sqrt{\frac{-2\beta_3 C-2\phi}{\beta_2}}}{w_1}+l_6\right)\right)\right)}{e^{-w\left(\frac{\nu\sqrt{\frac{-4\beta_3 C-4\phi}{\beta_2}}}{w}+l_2\right)} + r_2\cos\left(w_1\left(\frac{\nu\sqrt{\frac{-2\beta_3 C-2\phi}{\beta_2}}}{w_1}+l_6\right)\right) + r_1 e^{l_4 w}}. \tag{30}$$

Inserting Equation (30) into Equation (11) yields

$$U = -\frac{4\beta 1C\left(-\sqrt{\frac{-4\beta_3 C-4\phi}{\beta_2}}e^{-w\left(\frac{\nu\sqrt{\frac{-4\beta_3 C-4\phi}{\beta_2}}}{w}+l_2\right)} - r_2\sqrt{\frac{-2\beta_3 C-2\phi}{\beta_2}}\sin\left(w_1\left(\frac{\nu\sqrt{\frac{-2\beta_3 C-2\phi}{\beta_2}}}{w_1}+l_6\right)\right)\right)^2}{\phi\left(e^{-w\left(\frac{\nu\sqrt{\frac{-4\beta_3 C-4\phi}{\beta_2}}}{w}+l_2\right)} + r_2\cos\left(w_1\left(\frac{\nu\sqrt{\frac{-2\beta_3 C-2\phi}{\beta_2}}}{w_1}+l_6\right)\right) + r_1 e^{l_4 w}\right)^2}. \tag{31}$$

Inserting Equation (30) into Equation (31) and then into Equation (3), we get the solution for Υ and Ψ,

$$u(x,t) = e^{\zeta\eta(t)-\frac{\zeta^2 t}{2}}\left(-\frac{4\beta_1 C\left(-\sqrt{\frac{-4\beta_3 C-4\phi}{\beta_2}}e^{\lambda} - r_2\sqrt{\frac{-2\beta_3 C-2\phi}{\beta_2}}\sin(\Omega)\right)^2}{\phi\left(e^{\lambda}+r_2\cos(\Omega)+r_1 e^{l_4 w}\right)^2}\right)\left(t\phi + \frac{x^{\omega}}{\omega}\right), \tag{32}$$

$$v(x,t) = \frac{2e^{\zeta\eta(t)-\frac{\zeta^2 t}{2}}\left(-\sqrt{\frac{-4\beta_3 C-4\phi}{\beta_2}}e^{\lambda} - r_2\sqrt{\frac{-2\beta_3 C-2\phi}{\beta_2}}\sin(\Omega)\right)}{e^{\lambda}+r_2\cos(\Omega)+r_1 e^{l_4 w}}, \tag{33}$$

where $\Omega = w_1\left(\frac{\sqrt{\frac{-2\beta_3 C-2\phi}{\beta_2}}\left(t\phi+\frac{x^{\omega}}{\omega}\right)}{w_1}+l_6\right)$ and $\lambda = -w\left(\frac{\sqrt{\frac{-4\beta_3 C-4\phi}{\beta_2}}\left(t\phi+\frac{x^{\omega}}{\omega}\right)}{w}+l_2\right)$.

7. M-Shaped Rational Wave Solution

For the M-shaped rational wave solution, we use the following transformation [28]:

$$f = c_1^2 + c_2^2 + w_5, \qquad c_1 = w_1\nu + w_2, \qquad c_2 = w_3\nu + w_4. \tag{34}$$

Using Equation (34) into Equation (15), we get the following values for the solution:

$$w_1 = 0,\ w_4 = 0,\ w_5 = -\frac{3\beta_3 C w_2^2\phi + 3w_2^2\phi^2 - 4\beta_1\beta_3 w_3^2 - 8\beta_1\beta_4 w_3^2 + 3\beta_2 w_3^2\phi}{3(\phi(\beta_3 C + \phi))}. \tag{35}$$

Using Equation (35) into Equation (34) and then inserting into Equation (14), we get

$$V = \frac{4\nu w_3^2}{-\frac{3\beta_3 C w_2^2\phi + 3w_2^2\phi^2 - 4\beta_1\beta_3 w_3^2 - 8\beta_1\beta_4 w_3^2 + 3\beta_2 w_3^2\phi}{3\phi(\beta_3 C + \phi)} + w_2^2 + \nu^2 w_3^2}. \tag{36}$$

By using Equation (36) into Equation (11), we have

$$U = -\frac{16\beta_1 C\nu^2 w_3^4}{\phi\left(-\frac{3\beta_3 C w_2^2\phi + 3w_2^2\phi^2 - 4\beta_1\beta_3 w_3^2 - 8\beta_1\beta_4 w_3^2 + 3\beta_2 w_3^2\phi}{3\phi(\beta_3 C + \phi)} + w_2^2 + \nu^2 w_3^2\right)^2}. \tag{37}$$

Substituting Equation (36) into Equation (37) and then into Equation (3), we have the solution for Υ and Ψ,

$$u(x,t) = -\frac{16\beta_1 C w_3^4 e^{\zeta\eta(t) - \frac{\zeta^2 t}{2}}\left(t\phi + \frac{x^\omega}{\omega}\right)^2}{\phi\left(-\frac{3\beta_3 C w_2^2\phi + 3w_2^2\phi^2 - 4\beta_1\beta_3 w_3^2 - 8\beta_1\beta_4 w_3^2 + 3\beta_2 w_3^2\phi}{3\phi(\beta_3 C + \phi)} + w_3^2\left(t\phi + \frac{x^\omega}{\omega}\right)^2 + w_2^2\right)^2}, \tag{38}$$

$$v(x,t) = \frac{4w_3^2 e^{\zeta\eta(t) - \frac{\zeta^2 t}{2}}\left(t\phi + \frac{x^\omega}{\omega}\right)}{-\frac{3\beta_3 C w_2^2\phi + 3w_2^2\phi^2 - 4\beta_1\beta_3 w_3^2 - 8\beta_1\beta_4 w_3^2 + 3\beta_2 w_3^2\phi}{3\phi(\beta_3 C + \phi)} + w_3^2\left(t\phi + \frac{x^\omega}{\omega}\right)^2 + w_2^2}. \tag{39}$$

8. M-Shaped Rational Wave Solution with One Kink Wave

For an M-shaped rational wave solution with one kink wave, we assume the following f [29]:

$$f = c_1^2 + c_2^2 + r_1 e^{G_1} + w_5, \qquad c_1 = w_1\nu + w_2, \qquad c_2 = w_3\nu + w_4, \qquad G_1 = l_1\nu + l_2. \tag{40}$$

Using Equation (40) into Equation (15) and setting the coefficients of $x, t, e^{3l_1\nu+3l_2}, e^{2l_1\nu+2l_2}$ and $e^{l_1\nu+l_2}$ to zero, we have some values for the wave solution:

$$w_1 = 0, l_1 = \sqrt{-\frac{\beta_3 C + \phi}{\beta_2}}, w_4 = \frac{w_3\sqrt{-\frac{\beta_3 C+\phi}{\beta_2}}(4\beta_1\beta_3 + 8\beta_1\beta_4 - 9\beta_2\phi)}{15(\phi(\beta_3 C + \phi))}. \tag{41}$$

Evaluating Equation (41) into Equation (40) and then putting the result into Equation (14), we have

$$V = \frac{2\left(r_1\sqrt{\frac{\beta_3(-C)-\phi}{\beta_2}}e^{\nu\sqrt{\frac{\beta_3(-C)-\phi}{\beta_2}}+l_2} + 2w_3\left(\frac{w_3\sqrt{\frac{\beta_3(-C)-\phi}{\beta_2}}(4\beta_1\beta_3+8\beta_1\beta_4-9\beta_2\phi)}{15\phi(\beta_3C+\phi)} + \nu w_3\right)\right)}{r_1e^{\nu\sqrt{\frac{\beta_3(-C)-\phi}{\beta_2}}+l_2} + \left(\frac{w_3\sqrt{\frac{\beta_3(-C)-\phi}{\beta_2}}(4\beta_1\beta_3+8\beta_1\beta_4-9\beta_2\phi)}{15\phi(\beta_3C+\phi)} + \nu w_3\right)^2 + w_2^2 + w_5}. \tag{42}$$

Substituting Equation (42) into Equation (11), we get

$$U = -\frac{4\beta_1C\left(r_1\sqrt{\frac{\beta_3(-C)-\phi}{\beta_2}}e^{\nu\sqrt{\frac{\beta_3(-C)-\phi}{\beta_2}}+l_2} + 2w_3\left(\frac{w_3\sqrt{\frac{\beta_3(-C)-\phi}{\beta_2}}(4\beta_1\beta_3+8\beta_1\beta_4-9\beta_2\phi)}{15\phi(\beta_3C+\phi)} + \nu w_3\right)\right)^2}{\phi\left(r_1e^{\nu\sqrt{\frac{\beta_3(-C)-\phi}{\beta_2}}+l_2} + \left(\frac{w_3\sqrt{\frac{\beta_3(-C)-\phi}{\beta_2}}(4\beta_1\beta_3+8\beta_1\beta_4-9\beta_2\phi)}{15\phi(\beta_3C+\phi)} + \nu w_3\right)^2 + w_2^2 + w_5\right)^2}. \tag{43}$$

Evaluating Equations (42) and (43) into Equation (3), we obtain the solutions given below

$$u(x,t) = -\frac{4\beta_1Ce^{\zeta\eta(t)-\frac{\zeta^2t}{2}}\left(r_1\sqrt{\frac{\beta_3(-C)-\phi}{\beta_2}}e^{\sqrt{\frac{\beta_3(-C)-\phi}{\beta_2}}\left(t\phi+\frac{x^{\omega}}{\omega}\right)+l_2} + 2w_3(\Pi)\right)^2}{\phi\left(r_1e^{\sqrt{\frac{\beta_3(-C)-\phi}{\beta_2}}\left(t\phi+\frac{x^{\omega}}{\omega}\right)+l_2} + (\Pi)^2 + w_2^2 + w_5\right)^2}, \tag{44}$$

$$v(x,t) = \frac{2e^{\zeta\eta(t)-\frac{\zeta^2t}{2}}\left(r_1\sqrt{\frac{\beta_3(-C)-\phi}{\beta_2}}e^{\sqrt{\frac{\beta_3(-C)-\phi}{\beta_2}}\left(t\phi+\frac{x^{\omega}}{\omega}\right)+l_2} + 2w_3(\Pi)\right)}{r_1e^{\sqrt{\frac{\beta_3(-C)-\phi}{\beta_2}}\left(t\phi+\frac{x^{\omega}}{\omega}\right)+l_2} + (\Pi)^2 + w_2^2 + w_5}, \tag{45}$$

where $\Pi = \frac{w_3\sqrt{\frac{\beta_3(-C)-\phi}{\beta_2}}(4\beta_1\beta_3+8\beta_1\beta_4-9\beta_2\phi)}{15\phi(\beta_3C+\phi)} + w_3\left(t\phi + \frac{x^{\omega}}{\omega}\right)$.

9. M-Shaped Rational Wave Solution with Two Kink Waves

For the M-shaped rational wave solution with two kink waves, we assume the following ansatz [30]:

$$\begin{aligned} f &= c_1^2 + c_2^2 + r_1e^{G_1} + r_2e^{G_2} + w_5, \\ c_1 &= w_1\nu + w_2, \qquad c_2 = w_3\nu + w_4, \\ G_1 &= l_1\nu + l_2, \qquad G_2 = l_3\nu + l_4. \end{aligned} \tag{46}$$

Inserting Equation (46) into Equation (15) and setting the coefficients of x, t, $e^{3l_1\nu+3l_2}$, $e^{2l_1\nu+2l_2}$, $e^{l_1\nu+l_2}$, $e^{3l_3\nu+3l_4}$, $e^{2l_3\nu+2l_4}$, $e^{l_3\nu+l_4}$, $e^{2l_1\nu+2l_2+l_3\nu+l_4}$, $e^{l_1\nu+l_2+2l_3\nu+2l_4}$, $e^{l_1\nu+l_2+l_3\nu+l_4}$ to zero, we get some values for the wave solution:

$$l_3 = 0, w_1 = 0, w_5 = -\frac{\beta_3Cw_2^2 + 3\beta_3Cw_4^2 + w_2^2\phi - 3\beta_2w_3^2 + 3w_4^2\phi}{\beta_3C + \phi}. \tag{47}$$

Putting Equation (47) into Equation (46) and then inserting into Equation (14), we get

$$V = \frac{2\left(l_1 r_1 e^{l_1\nu+l_2} + 2w_3(\nu w_3 + w_4)\right)}{\frac{\beta_3(-C)w_2^2 - 3\beta_3 C w_4^2 - w_2^2\phi + 3\beta_2 w_3^2 - 3w_4^2\phi}{\beta_3 C+\phi} + r_1 e^{l_1\nu+l_2} + e^{l_4} r_2 + w_2^2 + (\nu w_3 + w_4)^2}. \quad (48)$$

Inserting Equation (48) into Equation (11) yields

$$U = -\frac{4\beta 1 C\left(l_1 r_1 e^{l_1\nu+l_2} + 2w_3(\nu w_3 + w_4)\right)^2}{\phi\left(\frac{\beta_3(-C)w_2^2 - 3\beta_3 C w_4^2 - w_2^2\phi + 3\beta_2 w_3^2 - 3w_4^2\phi}{\beta_3 C+\phi} + r_1 e^{l_1\nu+l_2} + e^{l_4} r_2 + w_2^2 + (\nu w_3 + w_4)^2\right)^2}. \quad (49)$$

Then, putting Equations (48) and (49) into Equation (3), we obtain

$$u(x,t) = -\frac{4\beta 1 C e^{\zeta\eta(t) - \frac{\zeta^2 t}{2}}\left(l_1 r_1 e^{l_1\left(t\phi + \frac{x^\omega}{\omega}\right)+l_2} + 2w_3\left(w_3\left(t\phi + \frac{x^\omega}{\omega}\right) + w_4\right)\right)^2}{\phi\left(\frac{\beta_3(-C)w_2^2 - 3\beta_3 C w_4^2 - w_2^2\phi + 3\beta_2 w_3^2 - 3w_4^2\phi}{\beta_3 C+\phi} + r_1 e^{l_1\left(t\phi + \frac{x^\omega}{\omega}\right)+l_2} + e^{l_4} r_2 + \left(w_3\left(t\phi + \frac{x^\omega}{\omega}\right) + w_4\right)^2 + w_2^2\right)^2}, \quad (50)$$

$$v(x,t) = \frac{2e^{\zeta\eta(t) - \frac{\zeta^2 t}{2}}\left(l_1 r_1 e^{l_1\left(t\phi + \frac{x^\omega}{\omega}\right)+l_2} + 2w_3\left(w_3\left(t\phi + \frac{x^\omega}{\omega}\right) + w_4\right)\right)}{\frac{\beta_3(-C)w_2^2 - 3\beta_3 C w_4^2 - w_2^2\phi + 3\beta_2 w_3^2 - 3w_4^2\phi}{\beta_3 C+\phi} + r_1 e^{l_1\left(t\phi + \frac{x^\omega}{\omega}\right)+l_2} + e^{l_4} r_2 + \left(w_3\left(t\phi + \frac{x^\omega}{\omega}\right) + w_4\right)^2 + w_2^2}. \quad (51)$$

10. M-Shaped Interaction with Rogue and Kink Waves

For the M-shaped interaction with rogue and kink waves, we assume the following f [29]:

$$\begin{aligned} f &= c_1^2 + c_2^2 + +r_1\cosh(G_1) + r_2 e^{G_2} + w_5, \\ c_1 &= w_1\nu + w_2, \qquad c_2 = w_3\nu + w_4, \\ G_1 &= l_1\nu + l_2, \qquad G_2 = l_3\nu + l_4. \end{aligned} \quad (52)$$

By using Equation (52) into Equation (15) and setting the coefficients of $x, t, e^{3l_3\nu+3l_4}$, $e^{2l_3\nu+2l_4}$, $e^{l_3\nu+l_4}, \cosh(l_1\nu + l_2), \cosh(l_1\nu + l_2), e^{l_3\nu+l_4}\cosh(l_1\nu + l_2), \cosh^2(l_1\nu + l_2)$, $\sinh(l_1\nu + l_2)$, $e^{2l_3\nu+2l_4}\sinh(l_1\nu + l_2), e^{l_3\nu+l_4}\sinh(l_1\nu + l_2), \sinh(l_1\nu + l_2)\cosh(l_1\nu + l_2)$, $\sinh(l_1\nu + l_2)\cosh^2(l_1\nu + l_2), e^{l_3\nu+l_4}\sinh^2(l_1\nu + l_2), \sinh^2(l_1\nu + l_2)$ and $\sinh^3(l_1\nu + l_2)$ to zero, we are left with some values for the wave solution:

$$w_1 = 0,\ l_3 = \sqrt{-\frac{\beta_3 C + \phi}{\beta_2}},\ w_4 = \frac{w_3(4\beta_1\beta_3 - 9\beta_2\phi)\sqrt{-\frac{\beta_3 C+\phi}{\beta_2}}}{15(\phi(\beta_3 C + \phi))}. \quad (53)$$

Putting Equation (53) into Equation (52) and then into Equation (14), we have the solution

$$V = \frac{2\left(\xi e^{\nu\sqrt{\frac{\beta_3(-C)-\nu}{\beta_2}}+l_4} + 2(\chi)(\Delta + w_3) + l_1 r_1\sinh(l_1\nu + l_2)\right)}{r_2 e^{\nu\sqrt{\frac{\beta_3(-C)-\nu}{\beta_2}}+l_4} + (\chi)^2 + r_1\cosh(l_1\nu + l_2) + w_2^2 + w_5}, \quad (54)$$

$$U = -\frac{4\beta_1 C\left(\xi e^{\nu\sqrt{\frac{\beta_3(-C)-\nu}{\beta_2}}+l_4} + 2(\chi)(\Delta + w_3) + l_1 r_1 \sinh(l_1\nu + l_2)\right)^2}{\phi\left(r_2 e^{\nu\sqrt{\frac{\beta_3(-C)-\nu}{\beta_2}}+l_4} + (\chi)^2 + r_1\cosh(l_1\nu + l_2) + w_2^2 + w_5\right)^2}, \tag{55}$$

where $\xi = r_2\left(\sqrt{\frac{\beta_3(-C)-\nu}{\beta_2}} - \frac{\nu}{2\beta_2\sqrt{\frac{\beta_3(-C)-\nu}{\beta_2}}}\right)$, $\chi = \frac{w_3(4\beta_1\beta_3 - 9\beta_2\nu)\sqrt{\frac{\beta_3(-C)-\nu}{\beta_2}}}{15\nu(\beta_3 C+\nu)} + \nu w_3$ and $\Delta = -\frac{w_3(4\beta_1\beta_3-9\beta_2\nu)\sqrt{\frac{\beta_3(-C)-\nu}{\beta_2}}}{15\nu^2(\beta_3C+\nu)} - \frac{w_3(4\beta_1\beta_3-9\beta_2\nu)}{30\beta_2\nu(\beta_3C+\nu)\sqrt{\frac{\beta_3(-C)-\nu}{\beta_2}}} - \frac{w_3(4\beta_1\beta_3-9\beta_2\nu)\sqrt{\frac{\beta_3(-C)-\nu}{\beta_2}}}{15\nu(\beta_3C+\nu)^2} - \frac{3\beta_2 w_3\sqrt{\frac{\beta_3(-C)-\nu}{\beta_2}}}{5\nu(\beta_3C+\nu)}$.

Evaluating Equations (54) and (55) into Equation (3), we obtain

$$u(x,t) = -\frac{4\beta_1 C e^{\zeta\eta(t)-\frac{\zeta^2 t}{2}}\left(r_2\left(\sqrt{\frac{-\beta_3 C - t\phi - \frac{x^\omega}{\omega}}{\beta_2}} - \frac{t\phi + \frac{x^\omega}{\omega}}{2\beta_2\sqrt{\frac{-\beta_3 C - t\phi - \frac{x^\omega}{\omega}}{\beta_2}}}\right)e^{\lambda} + 2(\Gamma - \Lambda)(\varrho) + l_1 r_1\sinh(\theta)\right)^2}{\phi\left(r_2 e^{\lambda} + (\varrho)^2 + r_1\cosh(\theta) + w_2^2 + w_5\right)^2}, \tag{56}$$

$$v(x,t) = \frac{2e^{\zeta\eta(t)-\frac{\zeta^2 t}{2}}\left(r_2\left(\sqrt{\frac{-\beta_3 C - t\phi - \frac{x^\omega}{\omega}}{\beta_2}} - \frac{t\phi + \frac{x^\omega}{\omega}}{2\beta_2\sqrt{\frac{-\beta_3 C - t\phi - \frac{x^\omega}{\omega}}{\beta_2}}}\right)e^{(\lambda)} + 2(\Gamma + \Lambda)(\varrho) + l_1 r_1\sinh(\theta)\right)}{r_2 e^{(\lambda)} + (\varrho)^2 + r_1\cosh(\theta) + w_2^2 + w_5}, \tag{57}$$

where $\varrho = \frac{w_3\sqrt{\frac{-\beta_3C-t\phi-\frac{x^\omega}{\omega}}{\beta_2}}\left(4\beta_1\beta_3 - 9\beta_2\left(t\phi+\frac{x^\omega}{\omega}\right)\right)}{15\left(t\phi+\frac{x^\omega}{\omega}\right)\left(\beta_3C+t\phi+\frac{x^\omega}{\omega}\right)} + w_3\left(t\phi + \frac{x^\omega}{\omega}\right)$, $\theta = l_1\left(t\phi + \frac{x^\omega}{\omega}\right) + l_2$,
$\Gamma = -\frac{w_3\left(4\beta_1\beta_3 - 9\beta_2\left(t\phi+\frac{x^\omega}{\omega}\right)\right)}{30\beta_2\left(t\phi+\frac{x^\omega}{\omega}\right)\left(\beta_3C+t\phi+\frac{x^\omega}{\omega}\right)\sqrt{\frac{-\beta_3C-t\phi-\frac{x^\omega}{\omega}}{\beta_2}}} - \frac{w_3\sqrt{\frac{-\beta_3C-t\phi-\frac{x^\omega}{\omega}}{\beta_2}}\left(4\beta_1\beta_3 - 9\beta_2\left(t\phi+\frac{x^\omega}{\omega}\right)\right)}{15\left(t\phi+\frac{x^\omega}{\omega}\right)^2\left(\beta_3C+t\phi+\frac{x^\omega}{\omega}\right)}$,
$\Lambda = -\frac{w_3\sqrt{\frac{-\beta_3C-t\phi-\frac{x^\omega}{\omega}}{\beta_2}}\left(4\beta_1\beta_3 - 9\beta_2\left(t\phi+\frac{x^\omega}{\omega}\right)\right)}{15\left(t\phi+\frac{x^\omega}{\omega}\right)\left(\beta_3C+t\phi+\frac{x^\omega}{\omega}\right)^2} - \frac{3\beta_2 w_3\sqrt{\frac{-\beta_3C-t\phi-\frac{x^\omega}{\omega}}{\beta_2}}}{5\left(t\phi+\frac{x^\omega}{\omega}\right)\left(\beta_3C+t\phi+\frac{x^\omega}{\omega}\right)} + w_3$,
$\lambda = \left(t\phi + \frac{x^\omega}{\omega}\right)\sqrt{\frac{-\beta_3C-t\phi-\frac{x^\omega}{\omega}}{\beta_2}} + l_4$.

11. M-Shaped Interaction with Periodic and Kink Waves

For the M-shaped interaction with periodic and kink waves, we use the given transformation [31–33]:

$$\begin{aligned} f &= c_1^2 + c_2^2 + +r_1\cos(G_1) + r_2 e^{G_2} + w_5, \\ c_1 &= w_1\nu + w_2, \qquad c_2 = w_3\nu + w_4, \\ G_1 &= l_1\nu + l_2, \qquad G_2 = l_3\nu + l_4. \end{aligned} \tag{58}$$

By using Equation (58) into Equation (15) and by comparing the coefficients of $x, t, e^{3l_3\nu+3l_4}, e^{2l_3\nu+2l_4}, e^{l_3\nu+l_4}, \cos(l_1\nu + l_2), e^{l_3\nu+l_4}\cos(l_1\nu + l_2), \cos^2(l_1\nu + l_2)$, $e^{l_3\nu+l_4}\cos^2(l_1\nu + l_2), e^{2l_3\nu+2l_4}\sin(l_1\nu + l_2), \sin(l_1\nu + l_2), e^{l_3\nu+l_4}\sin(l_1\nu + l_2)$, $e^{l_3\nu+l_4}\sin(l_1\nu +$

$l_2)\cos(l_1\nu+l_2), \sin(l_1\nu+l_2)\cos(l_1\nu+l_2),\ \sin(l_1\nu+l_2)\cos^2(l_1\nu+l_2)$ and $\sin^3(l_1\nu+l_2)$, we get some values for the wave solution:

$$l_3=0,\ w_1=-\frac{w_3w_4}{w_2}, \tag{59}$$
$$w_5=-\frac{\beta_3Cw_2^4+\beta_3Cw_2^2w_4^2+w_2^4\phi-3\beta_2w_2^2w_3^2+w_2^2w_4^2\phi-3\beta_2w_3^2w_4^2}{w_2^2(\beta_3C+\phi)}.$$

After inserting Equation (59) into Equation (58) and then inserting into Equation (14), we get

$$V=\frac{2\left(-\frac{\gamma}{w_2^2(\beta_3C+\nu)^2}+\frac{-w_2^4-w_2^2w_4^2}{w_2^2(\beta_3C+\nu)}-l_1r_1\sin(l_1\nu+l_2)-\frac{2w_3w_4\left(w_2-\frac{\nu w_3w_4}{w_2}\right)}{w_2}+2w_3(\nu w_3+w_4)\right)}{\frac{\gamma}{w_2^2(\beta_3C+\nu)}+r_1\cos(l_1\nu+l_2)+e^{l_4}r_2+\left(w_2-\frac{\nu w_3w_4}{w_2}\right)^2+(\nu w_3+w_4)^2}, \tag{60}$$

$$U=-\frac{4\beta_1C\left(-\frac{\gamma}{w_2^2(\beta_3C+\nu)^2}+\frac{-w_2^4-w_2^2w_4^2}{w_2^2(\beta_3C+\nu)}-l_1r_1\sin(l_1\nu+l_2)-\frac{2w_3w_4\left(w_2-\frac{\nu w_3w_4}{w_2}\right)}{w_2}+2w_3(\nu w_3+w_4)\right)^2}{\phi\left(\frac{\gamma}{w_2^2(\beta_3C+\nu)}+r_1\cos(l_1\nu+l_2)+e^{l_4}r_2+\left(w_2-\frac{\nu w_3w_4}{w_2}\right)^2+(\nu w_3+w_4)^2\right)^2}, \tag{61}$$

where $\gamma=\beta_3(-C)w_2^4-\beta_3Cw_2^2w_4^2-\nu w_2^4+3\beta_2w_2^2w_3^2-\nu w_2^2w_4^2+3\beta_2w_3^2w_4^2$.

By putting Equations (60) and (61), we have the following solutions

$$u(x,t)=-\frac{4\beta 1Ce^{\zeta\eta(t)-\frac{\zeta^2t}{2}}\left(-\frac{\varsigma}{w_2^2\left(\beta_3C+t\phi+\frac{x^\omega}{\omega}\right)^2}+\frac{-w_2^4-w_2^2w_4^2}{w_2^2\left(\beta_3C+t\phi+\frac{x^\omega}{\omega}\right)}-l_1r_1\sin(\varpi)-\frac{2w_3w_4(\psi)}{w_2}+2w_3(\kappa)\right)^2}{\phi\left(\frac{\varsigma}{w_2^2\left(\beta_3C+t\phi+\frac{x^\omega}{\omega}\right)}+r_1\cos(\varpi)+e^{l_4}r_2+(\psi)^2+(\kappa)^2\right)^2}, \tag{62}$$

$$v(x,t)=\frac{2e^{\zeta\eta(t)-\frac{\zeta^2t}{2}}\left(-\frac{\varsigma}{w_2^2\left(\beta_3C+t\phi+\frac{x^\omega}{\omega}\right)^2}+\frac{-w_2^4-w_2^2w_4^2}{w_2^2\left(\beta_3C+t\phi+\frac{x^\omega}{\omega}\right)}-l_1r_1\sin(\varpi)-\frac{2w_3w_4(\psi)}{w_2}+2w_3(\kappa)\right)}{\frac{\varsigma}{w_2^2\left(\beta_3C+t\phi+\frac{x^\omega}{\omega}\right)}+r_1\cos(\varpi)+e^{l_4}r_2+(\psi)^2+(\kappa)^2}, \tag{63}$$

where $\varsigma=\beta_3(-C)w_2^4-\beta_3Cw_2^2w_4^2-w_2^4\left(t\phi+\frac{x^\omega}{\omega}\right)-w_2^2w_4^2\left(t\phi+\frac{x^\omega}{\omega}\right)+3\beta_2w_2^2w_3^2+3\beta_2w_3^2w_4^2$, $\varpi=l_1\left(t\phi+\frac{x^\omega}{\omega}\right)+l_2$, $\psi=w_2-\frac{w_3w_4\left(t\phi+\frac{x^\omega}{\omega}\right)}{w_2}$ and $\kappa=w_3\left(t\phi+\frac{x^\omega}{\omega}\right)+w_4$.

12. Results and Discussion

Some researchers worked on the governing model such as Askar et al., who used the (G′/G)-expansion method to find exact solutions for the fractional–stochastic Drinfel'd–Sokolov–Wilson equations [18]. Qin and Yan worked on the applications of the coupled Drinfel'd–Sokolov–Wilson equation and also used an improved F-expansion method to find exact doubly periodic solutions in terms of the rational formal Jacobi elliptic function of nonlinear partial differential equations [34].

By selecting the appropriate values for the parameter, we were able to generate the desired types of solution that indicated a wave discrepancy. In Figures 1–28, we presented 3D, 2D, contour plots, respectively. In Figure 1, the M and W shape waves appeared with bright and dark faces. In Figure 2, we obtained a bright face and after some time, bright–dark faces appeared; in Figures 3 and 4, we represented 2D and contour plots of this wave solution by using the values $\beta_2=0.2, \beta_3=3.5, \zeta=0, l_2=0.03, Q=5, r_1=2.5, w_2=5$,

$w_3 = 0.3, w_4 = 0.9, \omega = 0.1$ and $\phi = 1.7$. According to Equation (26) and Equation (27), the periodic waves produced in Figures 5–8 varied in amplitude. In Figures 9–11, we can see one stripe soliton propagating at different times. The MSR solution was shown in Figures 12–16, where M-shaped waves appeared with bright–dark faces. In Figures 17a and 18a, one kink wave appeared and after some time, that one kink wave changed into the M-shaped wave shown in Figures 17b and 18b for Equation (44) and the remaining figures for that solution showed the 2D and contour plots. The MSR solution with two kink waves in Figures 19–21 with bright and dark faces was derived from Equations (50) and (51). For Equations (56) and (57) and Equations (62) and (63), the M-shaped interactions with RK and PK with some M-shaped dark and bright faces are shown in Figures 22–28.

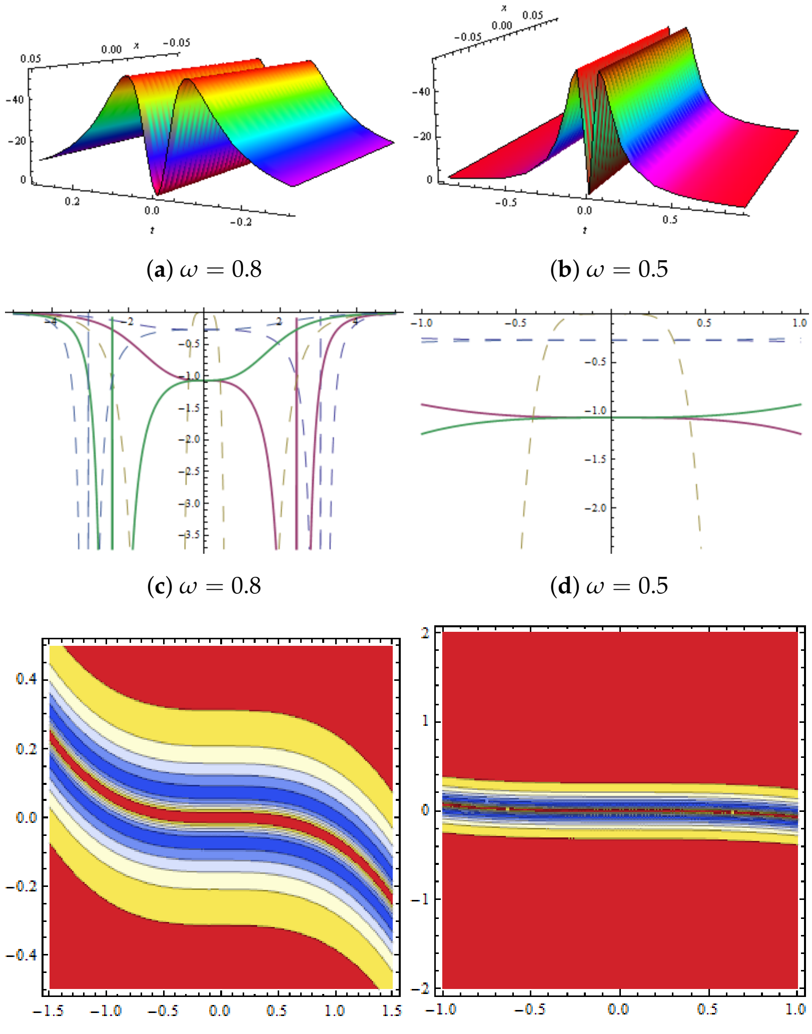

(**a**) $\omega = 0.8$ (**b**) $\omega = 0.5$

(**c**) $\omega = 0.8$ (**d**) $\omega = 0.5$

(**e**) $\omega = 0.8$ (**f**) $\omega = 0.5$

Figure 1. Show the behaviour of $u(x,t)$ in Equation (20), it is presented with $\beta_1 = 3.5$, $\beta_2 = 0.2$, $\beta_3 = 1.5, \zeta = 0, l_2 = 0.3$, $Q = 2, r_1 = 1.5$, $w_2 = 2.5, w_3 = 7.3$, $w_4 = 1.9$ and $\phi = 4.7$. (**a**,**b**) shows 3D graphs presenting bright and dark faces for $\omega = 0.8$ and $\omega = 0.5$ respectively, (**c**,**d**) show 2D graphs for bright and dark faces for $\omega = 0.8$ and $\omega = 0.5$ respectively. (**e**,**f**) show contour graphs for bright and dark faces for $\omega = 0.8$ and $\omega = 0.5$ respectively.

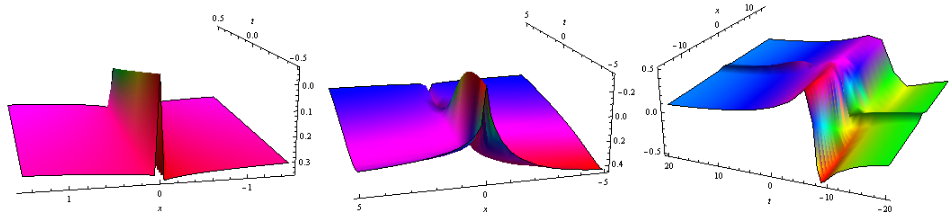

(**a**) $\omega = 2.0$ (**b**) $\omega = 5.0$ (**c**) $\omega = 7.0$

Figure 2. (**a**–**c**) show three-dimensional plots.

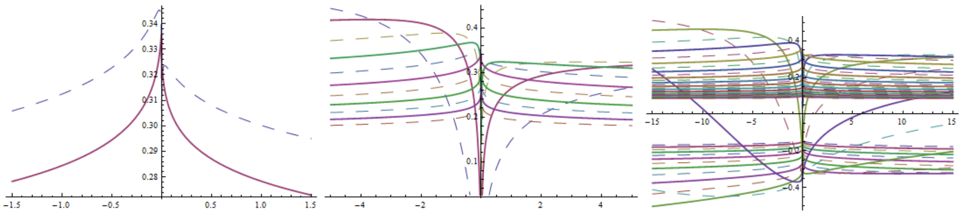

(**a**) $\omega = 2.0$ (**b**) $\omega = 5.0$ (**c**) $\omega = 7.0$

Figure 3. (**a**–**c**) show two-dimensional plots .

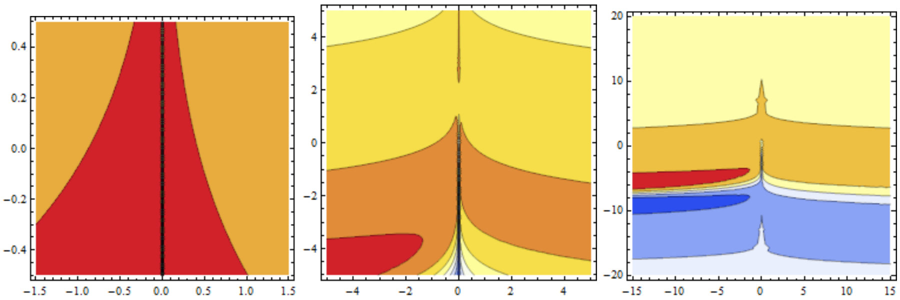

(**a**) $\omega = 2.0$ (**b**) $\omega = 5.0$ (**c**) $\omega = 7.0$

Figure 4. Graphical demonstration of the two-dimensional and three-dimensional representations and contour of solution $v(x,t)$ in Equation (21) with $\beta_2 = 0.2, \beta_3 = 3.5, \zeta = 0, l_2 = 0.03, Q = 5, r_1 = 2.5, w_2 = 5, w_3 = 0.3, w_4 = 0.9$, and $\phi = 1.7$. (**a**–**c**) show contour graphs.

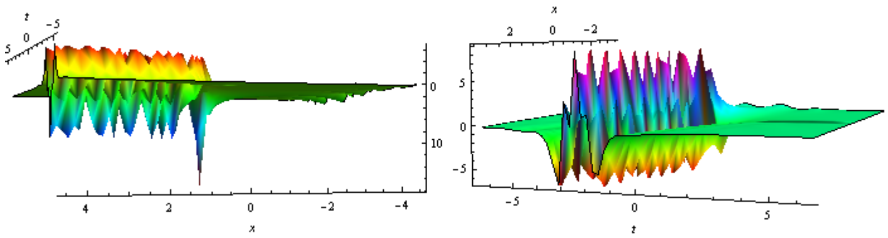

(**a**) $\omega = 3$ (**b**) , $\omega = 0.6$

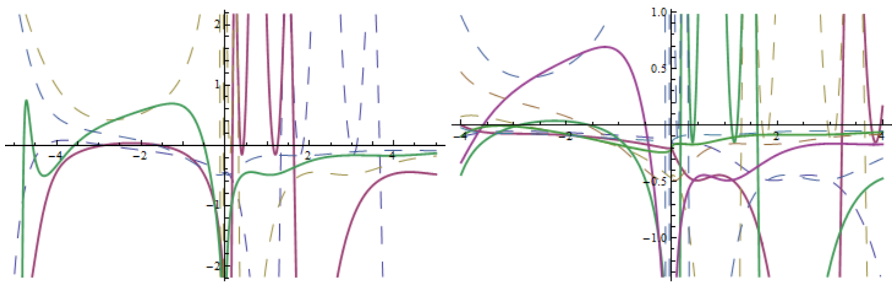

(**c**) , $\omega = 3$ (**d**) , $\omega = 0.6$

Figure 5. (**a**,**b**) show 3D plots and (**c**,**d**) show two-dimensional plots

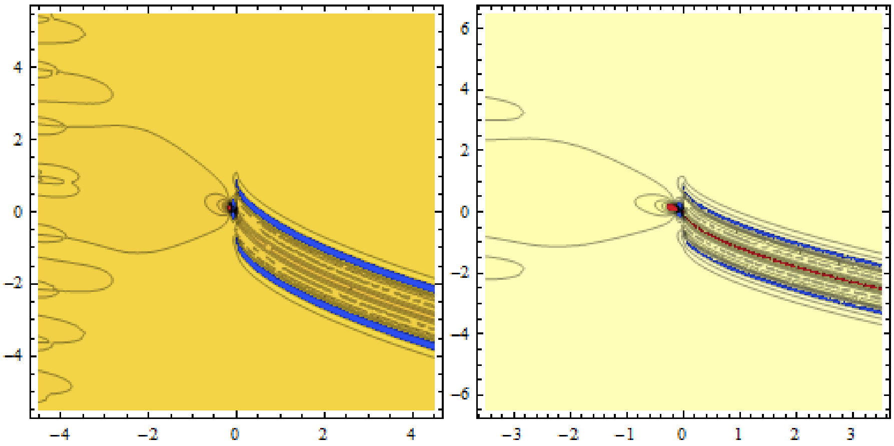

(**a**) $\omega = 3.0$ (**b**) $\omega = 0.6$

Figure 6. (**a**,**b**) show contour plots. The graphical behaviour of $u(x,t)$ in Equation (26) is presented with $\beta_1 = 0.3, \beta_2 = 0.2, \beta_3 = 0.5, \beta_4 = 0.4$, $\zeta = 0, l_1 = 0.3, l_2 = 0.1, l_4 = 4.5, l_5 = -0.5$, $Q = 1.2, r_1 = 2.5, r_2 = 3.2, w_2 = 0.2, w_3 = 3.1, w_4 = 1.5, w_5 = 5$ and $\phi = 1.4$.

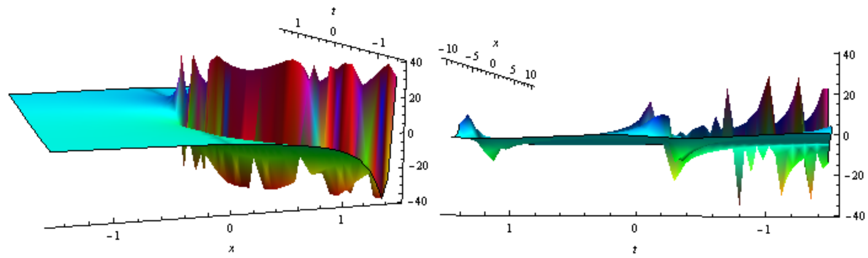

(**a**) $\omega = 3.0$ (**b**) $\omega = 0.6$

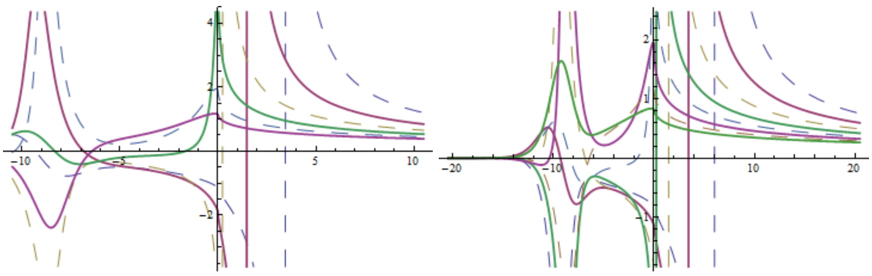

(**c**) $\omega = 3.0$ (**d**) $\omega = 0.6$

Figure 7. (**a**,**b**) show three-dimensional plots and (**c**,**d**) show two-dimensional plots.

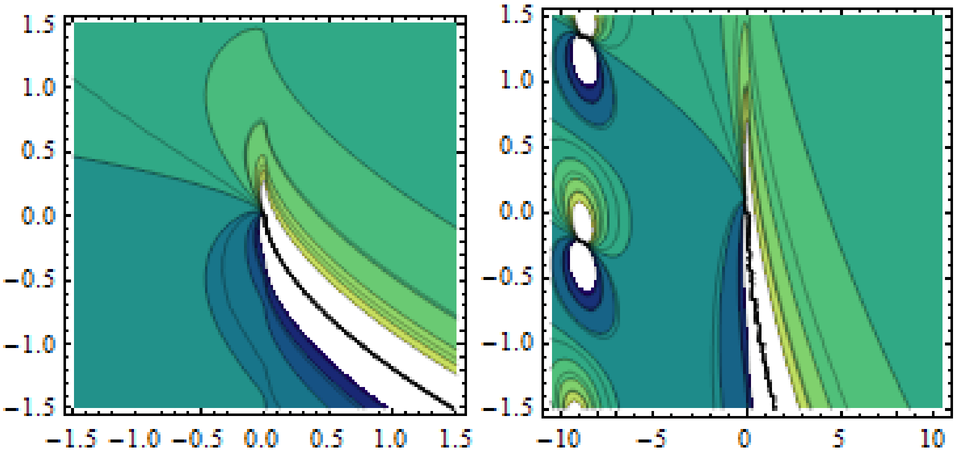

(**a**) $\omega = 3.0$ (**b**) $\omega = 0.6$

Figure 8. Graphical demonstration of solution $v(x,t)$ in Equation (27) presented with $\beta_1 = 0.3, \beta_2 = 0.2, \beta_3 = 0.5, \beta_4 = 0.04, \zeta = 0, l_1 = 0.1, l_2 = 0.01, l_4 = 4.4, l_5 = 0.5, Q = 1.2,$ $r_1 = 2.5, r_2 = 3.2, w_2 = 0.02, w_3 = 3.1, w_4 = 1.5, w_5 = 5$ and $\phi = 1.4$. (**a**,**b**) show contour plots for various values of ω.

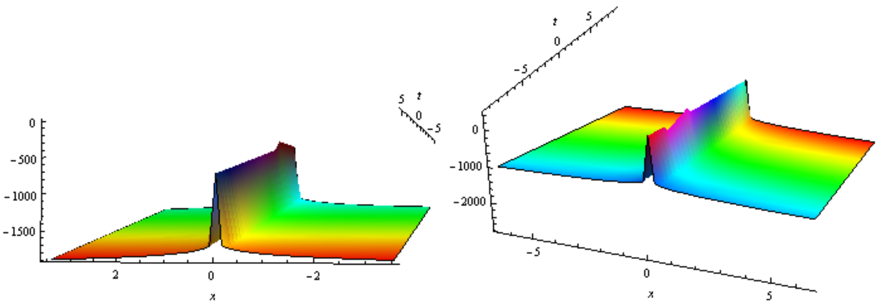

(**a**) $\omega = 2.0$ (**b**) $\omega = 0.04$

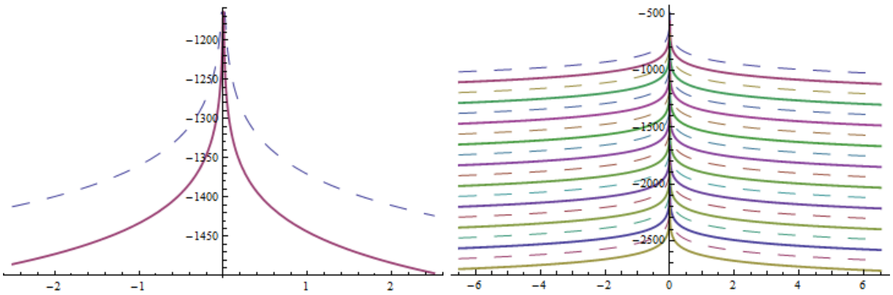

(**c**) $\omega = 2.0$ (**d**) $\omega = 0.04$

Figure 9. (**a**,**b**) show 3D plots and (**c**,**d**) show 2D plots.

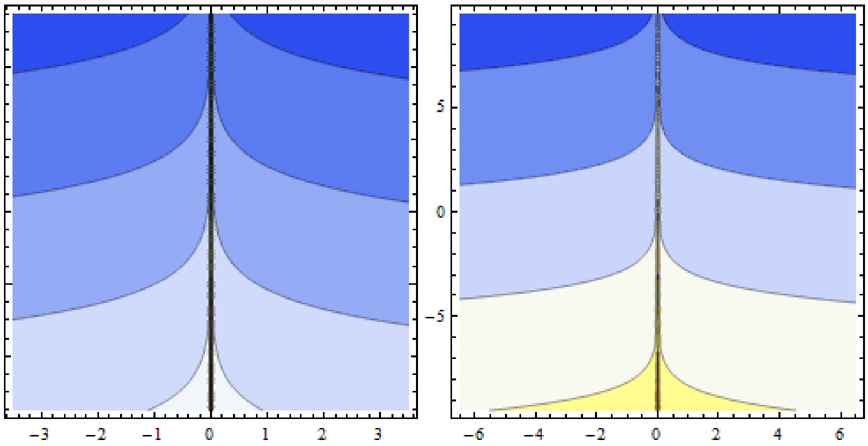

(**a**) $\omega = 2.0$ (**b**) $\omega = 0.04$

Figure 10. Dynamical behaviour of $u(x,t)$ in Equation (32) presented with $\beta_1 = 1.2$, $\beta_2 = 0.2$, $\beta_3 = 3.5, \zeta = 0, l_2 = 0.3, l_4 = 4.2, l_6 = 1.6, Q = 0.5, r_1 = 1.5, r_2 = 2.5, w = 3, w_1 = 2.5$, and $\phi = 1.3$. (**a**,**b**) show contour plots for various values of ω.

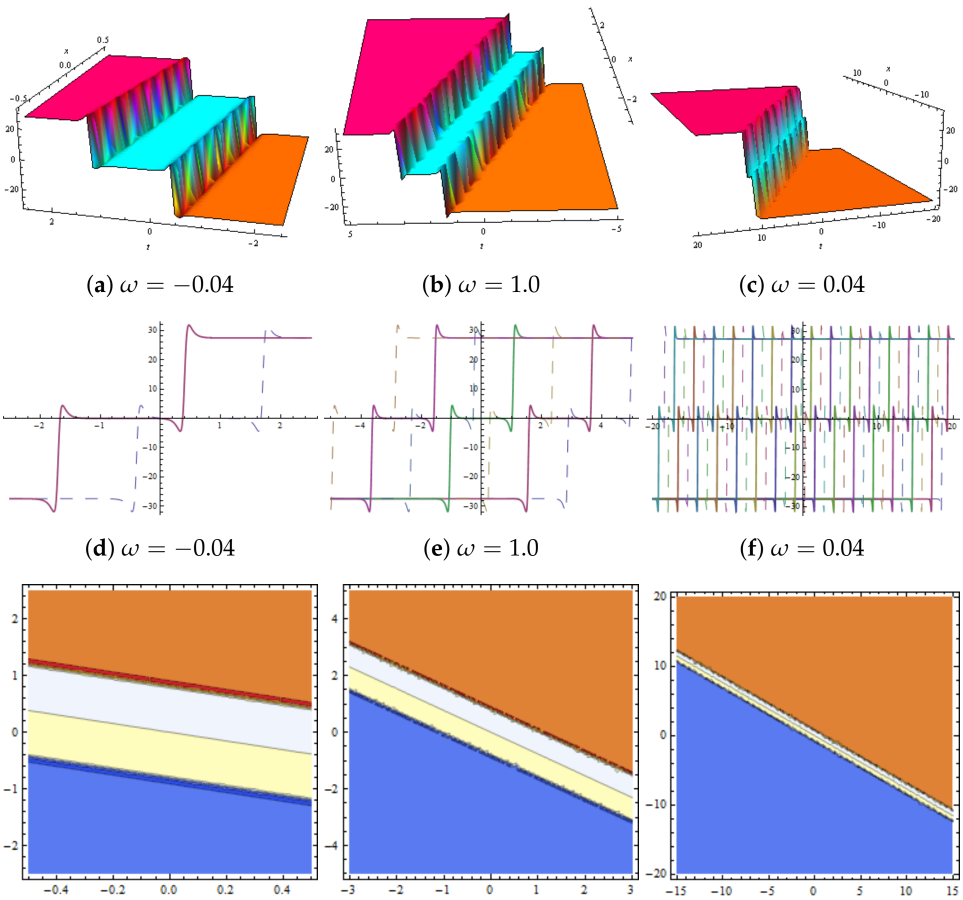

(**a**) $\omega = -0.04$ (**b**) $\omega = 1.0$ (**c**) $\omega = 0.04$

(**d**) $\omega = -0.04$ (**e**) $\omega = 1.0$ (**f**) $\omega = 0.04$

(**g**) $\omega = -0.04$ (**h**) 1.0 (**i**) $\omega = 0.04$

Figure 11. (**a**–**c**) show 3D graphs. Dynamical representation of solution $v(x,t)$ in Equation (33) with $\beta_2 = 0.2, \beta_3 = 3.5, \zeta = 0, l_2 = 0.03, Q = 5, r_1 = 2.5, w_2 = 5, w_3 = 0.3, w_4 = 0.9, \phi = 1.7$. (**d**–**f**) show 2D plots and (**g**–**i**) represent contour graphs for various values of ω.

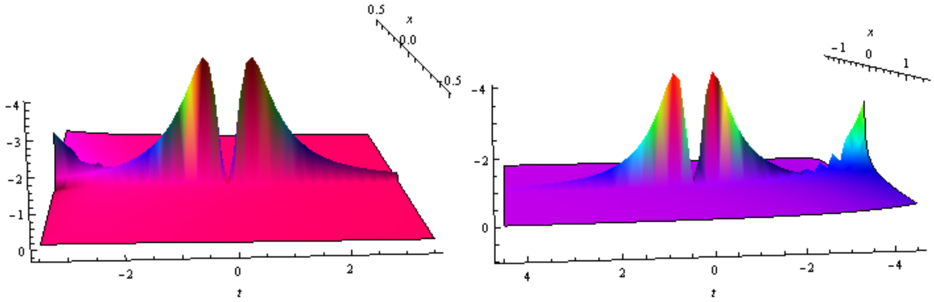

(**a**) $\omega = 0.1$ (**b**) $\omega = 0.6$

Figure 12. (**a**,**b**) show 3D plots.

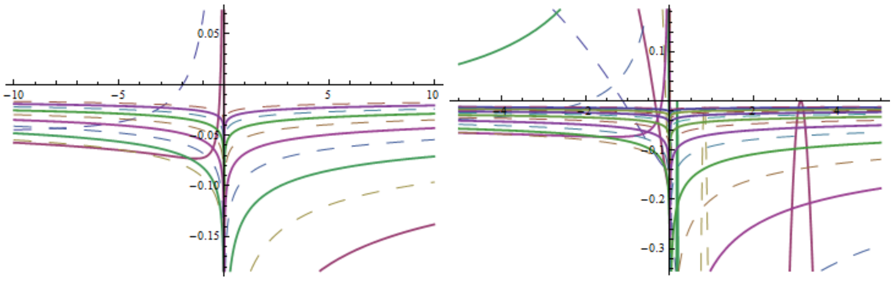

(**a**) $\omega = 0.1$ (**b**) $\omega = 0.6$

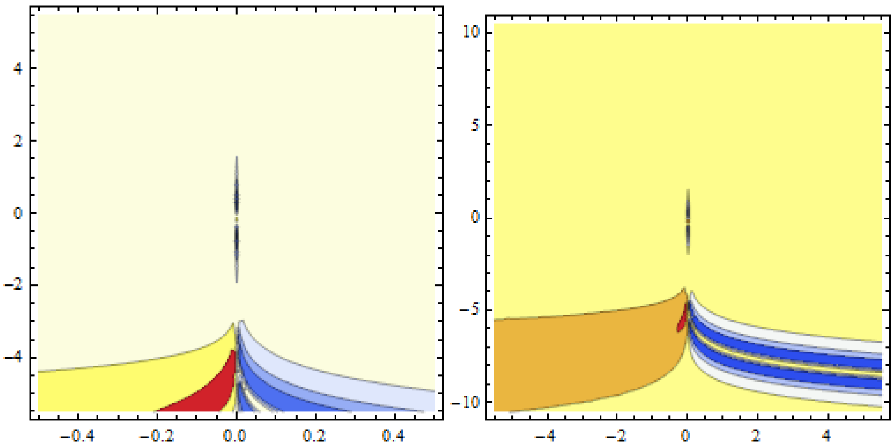

(**c**) $\omega = 0.1$ (**d**) $\omega = 0.6$

Figure 13. Dynamical behaviour of $u(x,t)$ in Equation (38) presented with $\beta_1 = 0.3, \beta_2 = 2.2, \beta_3 = 0.5, \beta_4 = 5.4, \zeta = 0, Q = 2, w_2 = 1.1, w_3 = 3.2$ and $\phi = 1.4$. (**a**,**b**) show 2D plots and (**c**,**d**) represent contour plots for different values of ω.

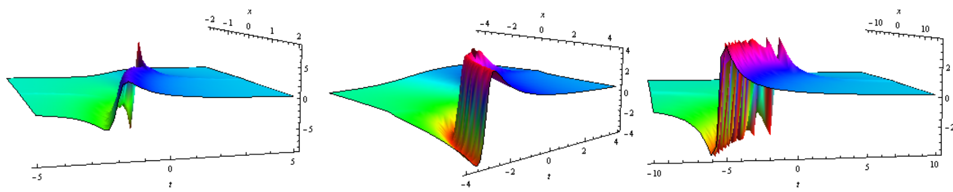

(**a**) $\omega = -1.5$ (**b**) $\omega = 1.0$ (**c**) $\omega = 1.5$

Figure 14. (**a**–**c**) show 3D plots.

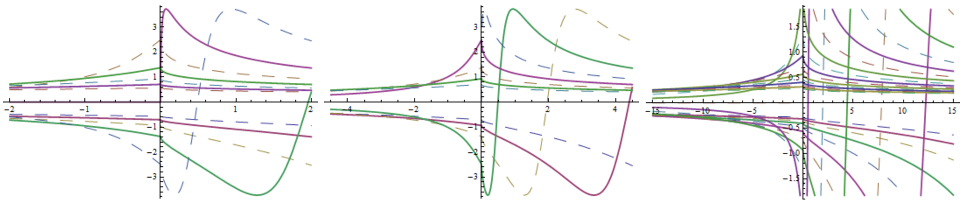

(**a**) $\omega = -1.5$ (**b**) $\omega = 1.0$ (**c**) $\omega = 1.5$

Figure 15. (**a**–**c**) show 2D plots.

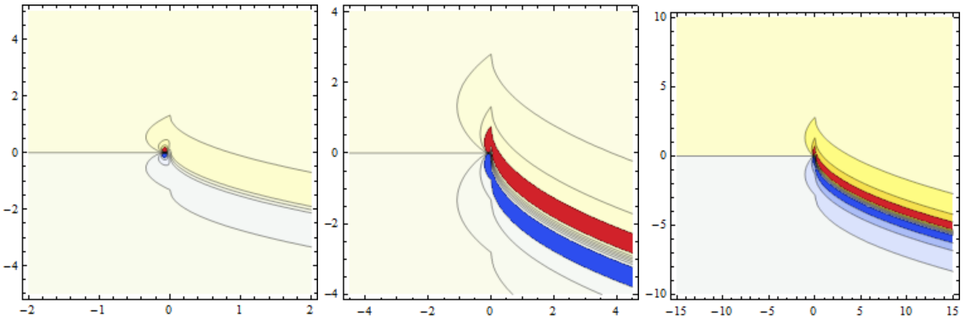

(**a**) $\omega = -1.5$ (**b**) $\omega = 1.0$ (**c**) $\omega = 1.5$

Figure 16. Behaviour of $v(x,t)$ in Equation (39) presented with $\beta_1 = 1.3, \beta_2 = 0.2, \beta_3 = 1.5, \beta_4 = 0.4, \zeta = 0, Q = 5.2, w_2 = 0.1, w_3 = 3$ and $\phi = 1.4$. (**a**–**c**) show contour graphs for various values of ω.

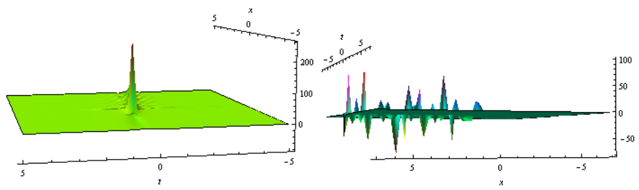

(**a**) $\omega = 0.8$ (**b**) $\omega = 2.0$

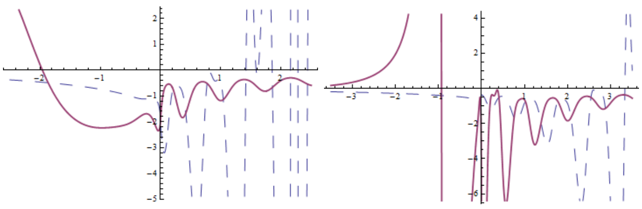

(**c**) $\omega = 0.8$ (**d**) $\omega = 2.0$

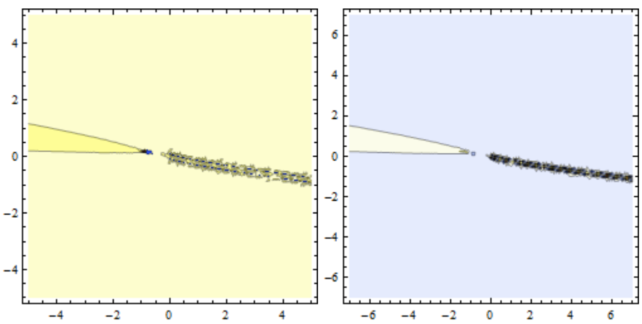

(**e**) $\omega = 0.8$ (**f**) $\omega = 2.0$

Figure 17. Dynamical demonstration of $u(x,t)$ in Equation (44) presented with $\beta_1 = 1.3, \beta_2 = 0.2, \beta_3 = 3.5, \beta_4 = 0.4, \zeta = 0, l_2 = 0.1, l_5 = 0.5, Q = 3.2, r_1 = 2.5, w_2 = 2, w_3 = 3.5, w_5 = 1.5$, and $\phi = 5.4$. (**a**,**b**) show 3D graph of lump wave, (**c**,**d**) represent 2D graph and (**e**,**f**) show contour plot.

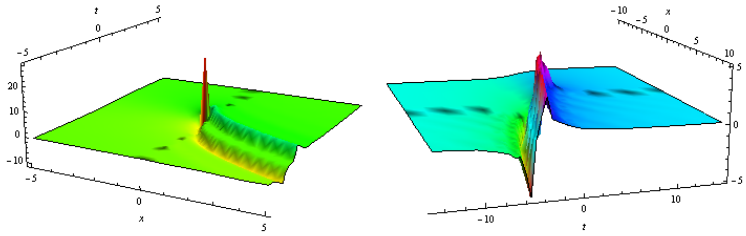

(**a**) $\omega = 0.6$ (**b**) $\omega = 1.5$

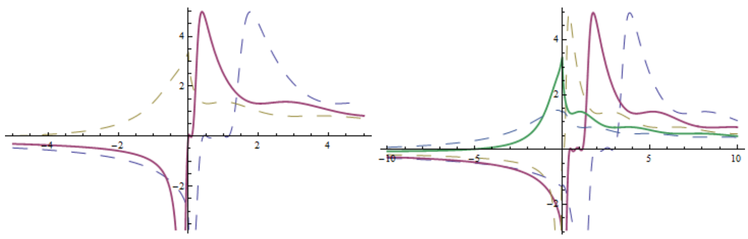

(**c**) $\omega = 0.6$ (**d**) $\omega = 1.5$

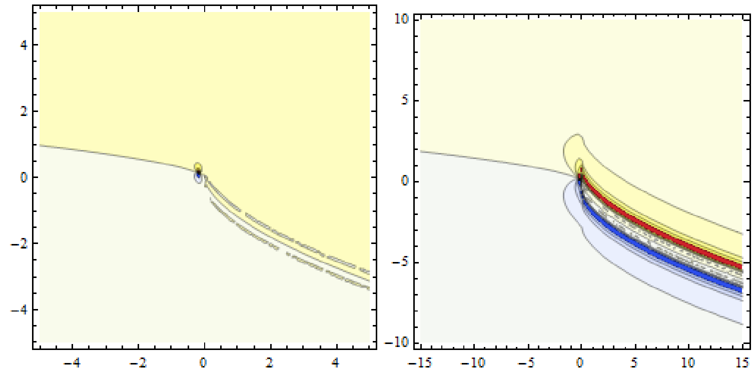

(**e**) $\omega = 0.6$ (**f**) $\omega = 1.5$

Figure 18. Dynamical behaviour of $v(x,t)$ in Equation (45) represented via $\beta_1 = 0.3$, $\beta_2 = 0.2$, $\beta_3 = 0.5, \beta_4 = 0.04, \zeta = 0, l_2 = 0.01, l_5 = 0.5, Q = 1.2, r_1 = 2.5, w_2 = 0.02, w_3 = 3.1$, and $\phi = 1.4$. (**a**,**b**) show 3D graph of lump wave, (**c**,**d**) represent 2D graph and (**e**,**f**) show contour plot for different values of ω.

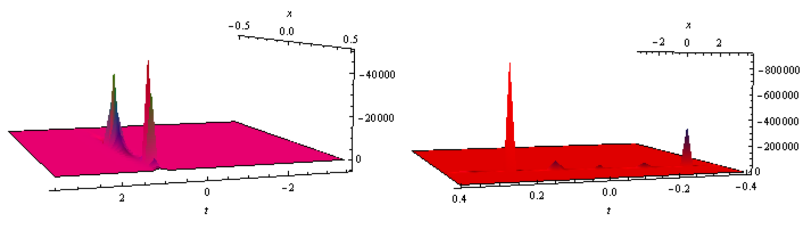

(**a**) $\omega = 1.5$ (**b**) $\omega = 3.5$

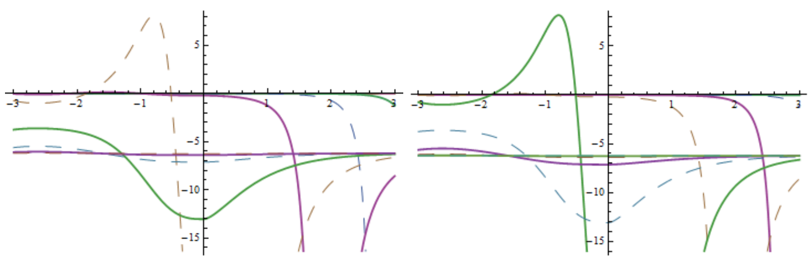

(**c**) $\omega = 1.5$ (**d**) $\omega = 3.5$

Figure 19. (**a**,**b**) show 3D plots and (**c**,**d**) show 2D plots.

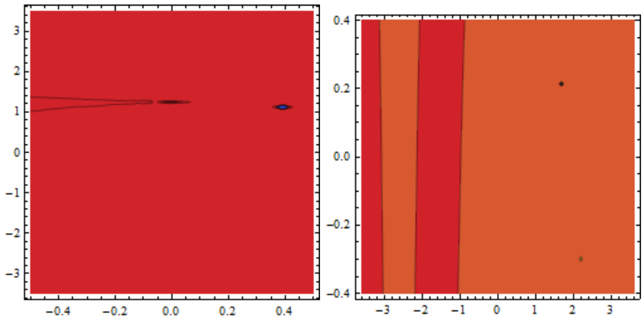

(**a**) $\omega = 1.5$ (**b**) $\omega = 3.5$

Figure 20. Dynamical demonstration of $u(x,t)$ in Equation (50) presented with $\beta_1 = 1.5, \beta_2 = 0.2$, $\beta_3 = 0.5, \zeta = 0, l_1 = 1.1, l_2 = 0.1, l_4 = 0.5, Q = 1.2, r_1 = 2.5, r_2 = 0.12, w_2 = 0.2, w_3 = 0.03$, $w_4 = 3.1$ and $\phi = 1.4$. (**a**,**b**) show contour plots for different ω.

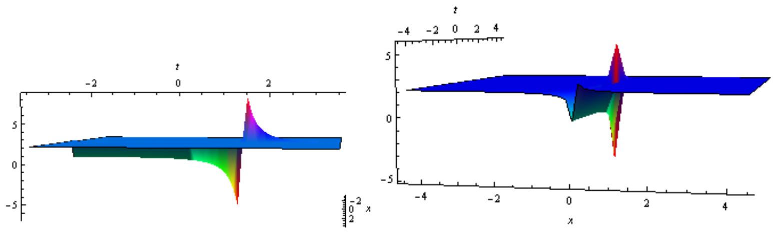

(**a**) $\omega = 0.09$ (**b**) $\omega = 0.04$

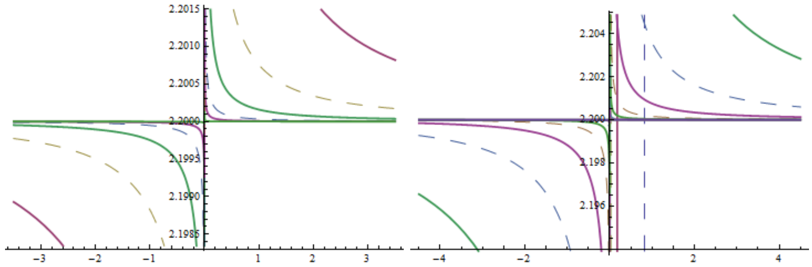

(**c**) $\omega = 0.09$ (**d**) $\omega = 0.04$

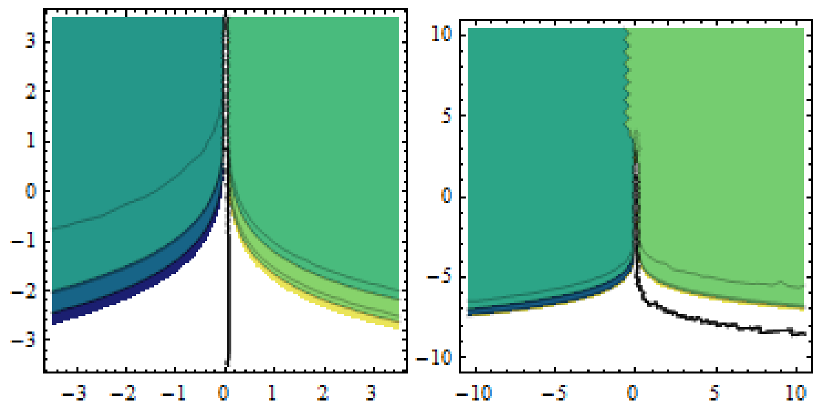

(**e**) $\omega = 0.09$ (**f**) $\omega = 0.04$

Figure 21. Graphical representation of solution $v(x,t)$ in Equation (51) with $\beta_2 = 0.2, \beta_3 = 0.5, \zeta = 0$, $l_1 = 1.1, l_2 = 0.01, l_4 = 0.5, Q = 1.2, r_1 = 2.5, r_2 = 0.12, w_2 = 0.02, w_3 = 0.03, w_4 = 3.1$, and $\phi = 1.4$. (**a**,**b**) show 3D graph of lump wave, (**c**,**d**) represent 2D graph and (**e**,**f**) show contour plot.

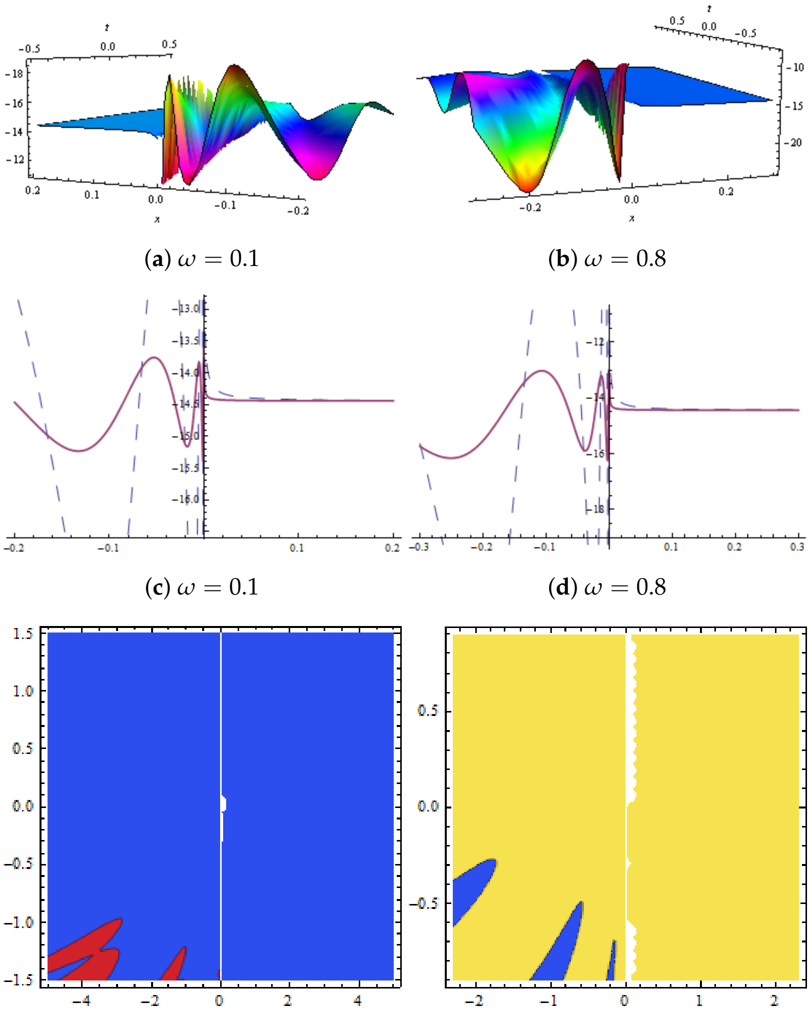

(**a**) $\omega = 0.1$ (**b**) $\omega = 0.8$

(**c**) $\omega = 0.1$ (**d**) $\omega = 0.8$

(**e**) $\omega = 0.1$ (**f**) $\omega = 0.8$

Figure 22. Graphical demonstration of $u(x,t)$ in Equation (56) presented with $\beta_1 = 0.3, \beta_2 = 1.2$, $\beta_3 = 0.5, \zeta = 0, l_1 = -1.8, l_2 = 0.05, l_4 = 0.01, Q = 5.2, r_1 = 2.5, r_2 = 1.3, w_2 = 0.1, w_3 = 3$, $w_4 = 1.9, w_5 = 1.2$ and $\phi = 1.4$. (**a**,**b**) show 3D graph, (**c**,**d**) represent 2D graph and (**e**,**f**) show contour plot.

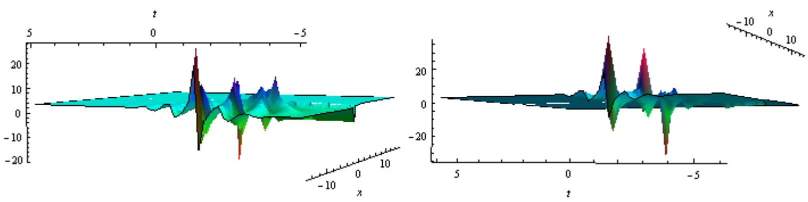

(**a**) $\omega = 0.1$ (**b**) $\omega = 0.8$

Figure 23. *Cont.*

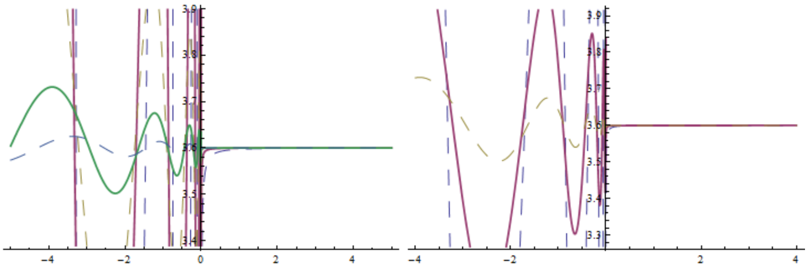

(**c**) $\omega = 0.1$ (**d**) $\omega = 0.8$

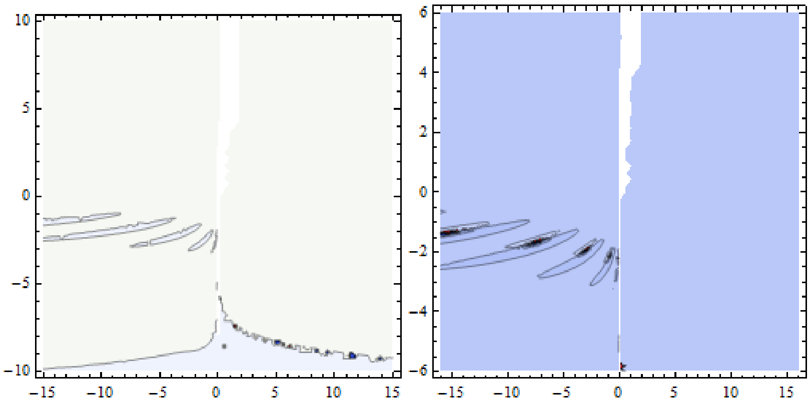

(**e**) $\omega = 0.1$ (**f**) $\omega = 0.8$

Figure 23. (**a**,**b**) show 3D graphs and (**c**,**d**) represent 2D graph. Dynamical presentation of solution $v(x,t)$ in Equation (57) with $\beta_1 = 0.3, \beta_2 = 1.2, \beta_3 = 0.5$, $\zeta = 0, l_1 = -1.8, l_2 = 0.05, l_4 = 0.01$, $Q = 5.2, r_1 = 2.5, r_2 = 1.3, w_2 = 0.1, w_3 = 3, w_4 = 1.9, w_5 = 1.2$ and $\phi = 1.4$. (**e**,**f**) show contour plot.

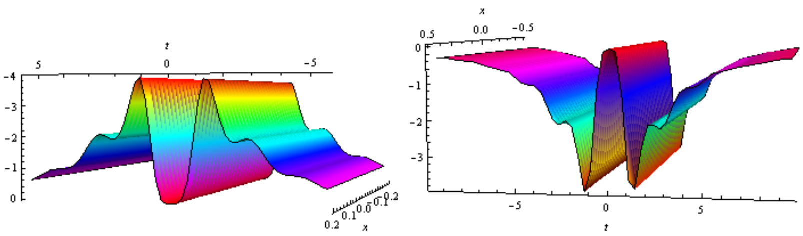

(**a**) $\omega = 4.5$ (**b**) $\omega = 2.5$

Figure 24. (**a**,**b**) show 3D plots.

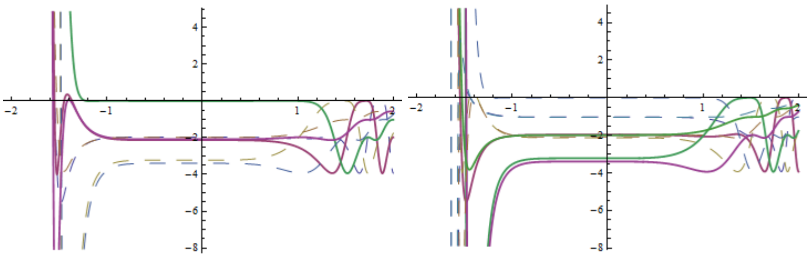

(**a**) $\omega = 4.5$ (**b**) $\omega = 2.5$

Figure 25. *Cont*.

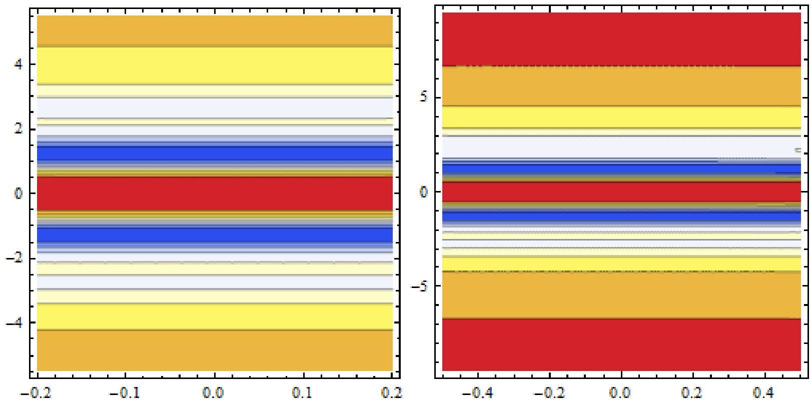

(**c**) $\omega = 4.5$ (**d**) $\omega = 2.5$

Figure 25. Graphical presentation of $u(x,t)$ in Equation (62) presented with $\beta_1 = 0.5, \beta_2 = 1.2, \beta_3 = 2.5, \zeta = 0, l_1 = 3, l_2 = 0.1, l_4 = 2, Q = 5, r_1 = 1.5, r_2 = 3.1, w_2 = 1.1, w_3 = 2.3, w_4 = 0.9$ and $\phi = 1.2$. (**a**,**b**) show 2D plot and (**c**,**d**) show contour graph.

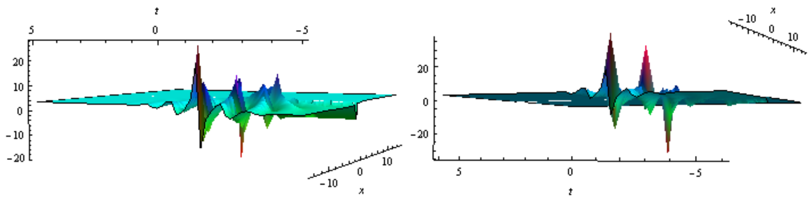

(**a**) $\omega = 0.4$ (**b**) $\omega = 0.1$

Figure 26. (**a**,**b**) show 3D plots.

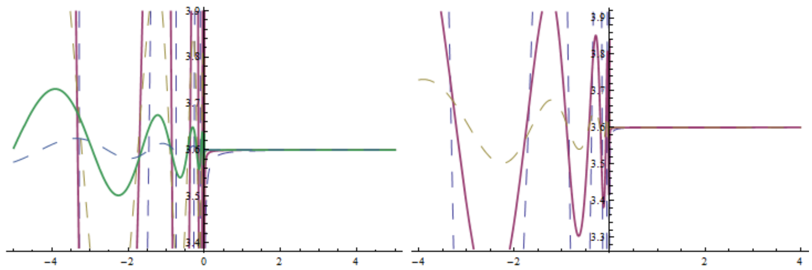

(**a**) $\omega = 0.4$ (**b**) $\omega = 0.1$

Figure 27. (**a**,**b**) show 2D plots.

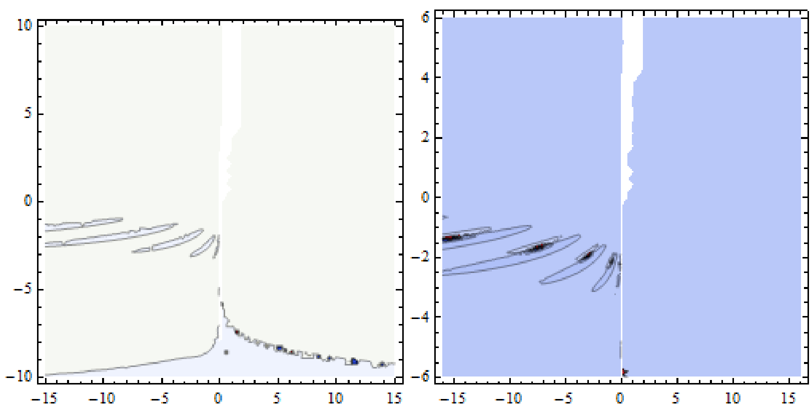

(**a**) $\omega = 0.4$ (**b**) 0.1

Figure 28. Dynamical presentation of solution $v(x,t)$ in Equation (63) with $\beta_2 = 0.2, \beta_3 = 3.5, \zeta = 0, l_1 = 0.03, l_2 = 0.01, l_4 = 2, Q = 5, r_1 = 4.5, r_2 = 2.1, w_2 = 0.1, w_3 = 4.3, w_4 = 1.9$ and $\phi = 1.2$. (**a**,**b**) show contour plot.

13. Conclusions

In this paper, we explored some wave solutions for stochastic–fractional Drinfel'd–Sokolov–Wilson. These equations are used in applied sciences, plasma physics, population dynamics, surface physics and mathematical physics. The obtained solutions were better and more useful and efficient for understanding a variety of significant physical phenomena. We acquired different types of solutions such as the periodic cross-rational wave solution, cross-kink rational wave solution, homoclinic breather wave solution, M-shaped rational wave solution, M-shaped rational wave solution with one kink wave, M-shaped rational wave solution with two kink waves, M-shaped interaction with rogue and kink waves, M-shaped interaction with periodic and kink waves. We also represented these wave solutions graphically.

Author Contributions: Conceptualization, S.T.R.R.; Methodology, S.T.R.R.; Writing—review & editing, S.A.M.A.; Supervision, A.R.S. All authors have read and agreed to the published version of the manuscript.

Funding: This research received no external funding.

Data Availability Statement: Not applicable.

Acknowledgments: The authors extend their appreciation to the Deanship for Research and Innovation, Ministry of Education in Saudi Arabia for funding this research work through the project number: IFP22UQU4290491DSR141.

Conflicts of Interest: The authors declare no conflict of interest.

References

1. Sahoo, S.; Ray, S.S.; Abdou, M.A.M.; Inc, M.; Chu, Y.M. New Soliton Solutions of Fractional Jaulent-Miodek System with Symmetry Analysis. *Symmetry* **2020**, *12*, 1001. [CrossRef]
2. Chu, Y.M.; Khan, M.S.; Abbas, M.; Ali, S.; Nazeer, W. On characterizing of bifurcation and stability analysis for time fractional glycolysis model. *Chaos Solitons Fractals* **2022**, *165*, 112804. [CrossRef]
3. Li, R.; İlhan, O.A.; Manafian, J.; Mahmoud, K.H.; Abotaleb, M.; Kadi, A. A Mathematical Study of the (3+1)-D Variable Coefficients Generalized Shallow Water Wave Equation with Its Application in the Interaction between the Lump and Soliton Solutions. *Mathematics* **2022**, *10*, 3074. [CrossRef]
4. Zhang, H.; Manafian, J.; Singh, G.; Ilhan, O.A.; Zekiy, A.O. N-lump and interaction solutions of localized waves to the (2 + 1)-dimensional generalized KP equation. *Results Phys.* **2021**, *25*, 104168. [CrossRef]
5. Zhang, M.; Xie, X.; Manafian, J.; Ilhan, O.A.; Singh, G. Characteristics of the new multiple rogue wave solutions to the fractional generalized CBS-BK equation. *J. Adv. Res.* **2022**, *38*, 131–142. [CrossRef]
6. Samraiz, M.; Mehmood, A.; Iqbal, S.; Naheed, S.; Rahman, G.; Chu, Y.-M. Generalized fractional operator with applications in mathematical physics. *Chaos Solitons Fractals* **2022**, *165 Pt 2*, 112830. [CrossRef]
7. Huang, L.; Manafian, J.; Singh, G.; Nisar, K.S. Mahyuddin K.M. Nasution, New lump and interaction soliton, N-soliton solutions and the LSP for the (3 + 1)-D potential-YTSF-like equation. *Results Phys.* **2021**, *29*, 104713. [CrossRef]
8. Gu, Y.; Zia, S.M.; Isam, M.; Manafian, J.; Hajar, A.; Abotaleb, M. Bilinear method and semi-inverse variational principle approach to the generalized (2+1)-dimensional shallow water wave equation. *Results Phys.* **2023**, *45*, 106213. [CrossRef]
9. Seadawy, A.R.; Rizvi, S.T.R.; Mustafa, B.; Ali, K.; Althubiti, S. Chirped periodic waves for an cubic quintic nonlinear Schrödinger equation with self steepening and higher order nonlinearities. *Chaos Solitons Fractals* **2022**, *156*, 111804. [CrossRef]
10. Seadawy, A.R.; Ahmad, S.; Rizvi, S.T.R.; Ali, K. Various forms of lumps and interaction solutions to generalized Vakhnenko Parkes equation arising from high-frequency wave propagation in electromagnetic physics. *J. Geom. Phys.* **2022**, *176*, 104507. [CrossRef]
11. Rizvi, S.T.R.; Seadawy, A.R.; Farrah, N.; Ahmad, S. Application of Hirota operators for controlling soliton interactions for Bose-Einstien condensate and quintic derivative nonlinear Schrödinger equation. *Chaos Solitons Fractals* **2022**, *159*, 112128. [CrossRef]
12. Seadawy, A.R.; Bilal, M.; Younis, M.; Rizvi, S.T.R.; Althobaiti, S.; Makhlouf, M.M. Analytical mathematical approaches for the double chain model of DNA by a novel computational technique. *Chaos Solitons Fractals* **2021**, *144*, 110669. [CrossRef]
13. Seadawy, A.R.; Younis, M.; Baber, M.Z.; Iqbal, M.S.; Rizvi, S.T.R. Nonlinear acoustic wave structures to the Zabolotskaya Khokholov dynamical model. *J. Geom. Phys.* **2022**, *175*, 104474. [CrossRef]
14. Jia, H.X.; Zuo, D.W.; Li, X.H.; Xiang, X.S. Breather, soliton and rogue wave of a two-component derivative nonlinear Schrödinger equation. *Phys. Lett.* **2021**, *405*, 127426. [CrossRef]
15. Rizvi, S.T.R.; Younis, M.; Younis, B.; Ahmad, M.O. Exact optical solitons in (n+1)dimensions under anti cubic law of nonlinerity. *Optik* **2018**, *156*, 479–486.
16. Prévôt, C.; Röckner, M. A Concise Course on Stochastic Partial Differential Equations. *Lect. Notes Math.* **2007**, *1905*, 105–148.
17. Imkeller, P.; Monahan, A.H. Conceptual stochastic climate models. *World Sci.* **2002**, *2*, 311–326. [CrossRef]

18. Al-Askar, F.M.; Cesarano, C.; Mohammed, W.W. The Analytical Solutions of Stochastic-Fractional Drinfel'd-Sokolov-Wilson Equations via (G'/G)-Expansion Method. *Symmetry* **2022**, *14*, 2105. [CrossRef]
19. Khalil, R.; Al Horani, M.; Yousef, A.; Sababheh, M. A new definition of fractional derivative. *J. Comput. Appl. Math.* **2014**, *264*, 65–70. [CrossRef]
20. Calin, O. *An Informal Introduction to Stochastic Calculus with Applications*; World Scientific Publication Co. Pte. Ltd.: Singapore, 2015; p. 332.
21. Hirota, R. Exact solution of the Korteweg-de Vries equation for multiple collisions of solitons. *Phys. Rev. Lett.* **1971**, *27*, 1192–1194. [CrossRef]
22. Yang, J.Y.; Ma, W.X.; Qin, Z. Lump and lump-soliton solutions to the (2+1)-dimensional Ito equation. *Anal. Math. Phys.* **2018**, *8*, 427–436. [CrossRef]
23. Seadawy, A.R.; Rizvi, S.T.; Ashraf, M.A.; Younis, M.; Hanif, M. Rational solutions and their interactions with kink and periodic waves for a nonlinear dynamical phenomenon. *Int. J. Mod. Phys.* **2021**, *35*, 2150236. [CrossRef]
24. Rizvi, S.T.R.; Seadawy, A.R.; Ashraf, M.; Younis, M. Breather, multi-wave, periodic-cross kink, M-shaped and interactions solutions for perturbed NLSE with quadratic cubic nonlinearity. *Opt. Quantum Electron.* **2021**, *53*, 631.
25. Manafian, J.; Ivatloo, B.M.; Abapour, M. Breather wave, periodic, and cross-kink solutions to the generalized Bogoyavlensky-Konopelchenko equation. *Math. Methods Appl. Sci.* **2020**, *43*, 1753–1774. [CrossRef]
26. Seadawy, A.R.; Rizvi, S.T.R.; Ashraf, M.A.; Younis, M.; Khaliq, A.; Balwanu, D. Rogue, multi-wave, homoclinic breather, M-shaped rational and periodic-kink solutions for a nonlinear model describing vibrations. *Results Phys.* **2021**, *29*, 104654.
27. Ahmed, S.; Seadawy, A.R.; Rizvi, S.T.R. Study of breathers, rougue waves and lump soliton for the nonlinear chains of atoms. *Opt. Quantum Electron.* **2022**, *54*, 320. [CrossRef]
28. Ahmed, I.; Seadawy, A.R.; Lu, D. *M*-shaped rational solitons and their interaction with kink waves in the Fokas–Lenells equation. *Phys. Scripta* **2019**, *94*, 055205. [CrossRef]
29. Ashraf, F.; Seadawy, A.R.; Rizvi, S.T.R.; Ali, K.; Ashraf, M.A. Multi-wave, M-shaped rational and interaction solutions for fractional nonlinear electrical transmission line equation. *J. Geom. Phys.* **2022**, *177*, 104503. [CrossRef]
30. Ali, I.; Seadawy, A.R.; Rizvi, S.T.R.; Younis, M.; Ali, K. Conserved quantities along with Painleve analysis and Optical solitons for the nonlinear dynamics of Heisenberg ferromagnetic spin chains model. *Int. J. Mod. Phys. B* **2020**, *34*, 2050283. [CrossRef]
31. Faridi, W.A.; Asjad, M.I.; Toseef, M. Analysis of propagating wave structures of the cold bosonic atoms in a zig-zag optical lattice via comparison with two different analytical techniques. *Opt. Quantum Electron.* **2022**, *54*, 773. [CrossRef]
32. Ren, B.; Lin, J.; Lou, Z.M. A new nonlinear equation with lump-soliton, lump-periodic, and lump-periodic-soliton solutions. *Complexity* **2019**, *2019*, 4072754. [CrossRef]
33. Rizvi, S.T.R.; Seadawy, A.R.; Younis, M.; Ali, K.; Iqbal, H. Lump-solition, lump-multisoliton and lump periodic solutions of generalized hyperelastic rod equation. *Mod. Phys.* **2021**, *35*, 2150188.
34. Qin, Z.X.; Yan, Z.H. An improved F-expansion method and its application to coupled Drinfel'd-Sokolov-Wilson equation. *Commun. Theor. Phys.* **2008**, *50*, 309–314.

Disclaimer/Publisher's Note: The statements, opinions and data contained in all publications are solely those of the individual author(s) and contributor(s) and not of MDPI and/or the editor(s). MDPI and/or the editor(s) disclaim responsibility for any injury to people or property resulting from any ideas, methods, instructions or products referred to in the content.